analytical chemistry

Review

pubs.acs.org/ac

Small-Molecule Fluorescent Probes for Imaging and Detection of Reactive Oxygen, Nitrogen, and Sulfur Species in Biological Systems

Xiaoyun Jiao,[†] Yong Li,[†] Jinye Niu,[†,‡] Xilei Xie,[†] Xu Wang,*[,†] and Bo Tang*[,†]

[†]College of Chemistry, Chemical Engineering and Materials Science, Collaborative Innovation Center of Functionalized Probes for Chemical Imaging in Universities of Shandong, Key Laboratory of Molecular and Nano Probes, Ministry of Education, Institute of Molecular and Nano Science, Shandong Normal University, Jinan 250014, P. R. China

[‡]School of Chemical Engineering, Shandong University of Technology, Zibo 255049, P. R. China

CONTENTS

Intracellular redox homeostasis provides broad implications in physiological and pathological fields. The disruption of redox

Special Issue: Fundamental and Applied Reviews in Analytical Chemistry 2018

Published: October 23, 2017

ACS Publications © 2017 American Chemical Society

DOI: 10.1021/acs.analchem.7b04234
Anal. Chem. 2018, 90, 533−555

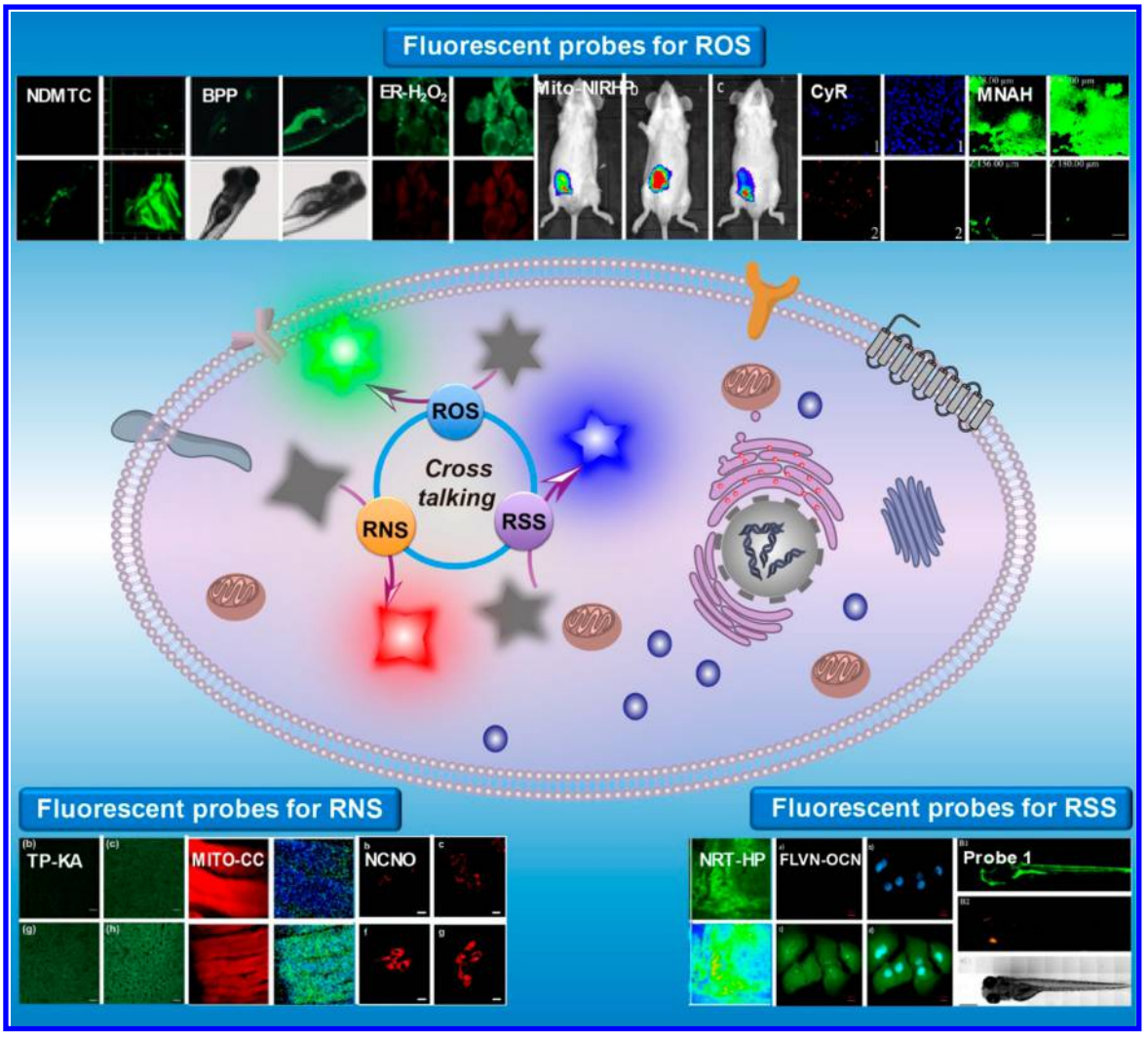

Figure 1. Fluorescent imaging of ROS, RNS, and RSS to elucidate their cross-talking in cells, tissues, and organisms. The representative data were reproduced from the following publications. NDMTC: Adapted from Zhu, B. C.; Li, P.; Shu, W.; Wang, X.; Liu, C. Y.; Wang, Y.; Wang, Z. K.; Wang, Y. W.; Tang, B. *Anal. Chem.* **2016**, *88*, 12532−12538 (ref 69). Copyright 2016 The American Chemical Society. BPP: Adapted from Xu, K. H.; Luan, D. R.; Wang, X. T.; Hu, B.; Liu, X. J.; Kong, F. P.; Tang. B. *Angew. Chem. Int. Ed.* **2016**, *55*, 12751−12754 (ref 78). Copyright 2016 Wiley. ER-H_2O_2: Adapted from Xiao, H. B.; Li, P.; Hu, X. F.; Shi, X. H.; Zhang, W.; Tang, B. *Chem. Sci.* **2016**, *7*, 6153−6159 (ref 25). Published by The Royal Society of Chemistry. Mito-NIRHP: Adapted from Xie, X. L.; Yang, X.; Wu, T. H.; Li, Y.; Li, M. M.; Tan, Q.; Wang, X.; Tang, B. *Anal. Chem.* **2016**, *88*, 8019−8025 (ref 35). Copyright 2016 The American Chemical Society. CyR: Adapted from Zhang, J. J.; Li, C. W.; Zhang, R.; Zhang, F. Y.; Liu, W.; Liu, X. Y.; Leeb, S. M.-Y.; Zhang, H. X. *Chem. Commun.* **2016**, *52*, 2679−2682 (ref 43). Copyright 2016 The Royal Society of Chemistry. MNAH: Adapted from Liu, H.-W.; Xu, S.; Wang, P.; Hu, X.-X.; Zhang, J.; Yuan, L.; Zhang, X.-B.; Tan, W. H. *Chem. Commun.* **2016**, *52*, 12330−12333 (ref 50). Copyright 2016 The Royal Society of Chemistry. TP-KA: Adapted from Li, Y.; Xie, X. L.; Yang, X.; Li, M. M.; Jiao, X. Y.; Sun, Y. H.; Wang, X.; Tang, B. *Chem. Sci.* **2017**, *8*, 4006−4011 (ref 90). Published by The Royal Society of Chemistry. MITO-CC: Adapted from Cheng, D.; Pan, Y.; Wang, L.; Zeng, Z. B.; Yuan, L.; Zhang, X. B.; Chang, Y.-T. *J. Am. Chem. Soc.* **2017**, *139*, 285−292 (ref 93). Copyright 2017 The American Chemical Society. NCNO: Adapted from Mao, Z. Q.; Jiang, H.; Li, Z.; Zhong, C.; Zhang, W.; Liu Z. H. *Chem. Sci.* **2017**, *8*, 4533−4538 (ref 104). Published by The Royal Society of Chemistry. Probe 1: Adapted from Yue, Y. K.; Huo, F. J.; Ning, P.; Zhang, Y. B.; Chao, J. B.; Meng, X. M.; Yin, C. X. *J. Am. Chem. Soc.* **2017**, *139*, 3181−3185 (ref 131). Copyright 2017 The American Chemical Society. FLVN-OCN: Adapted from Karakuş, E.; Üçüncü, M.; Emrullahoğlu, M. *Anal. Chem.* **2016**, *88*, 1039−1043 (ref 158). Copyright 2016 The American Chemical Society. NRT-HP: Adapted from Han, Q. X.; Mou, Z. L.; Wang, H. H.; Tang, X. L.; Dong, Z.; Wang, L.; Dong, X.; Liu, W. S. *Anal. Chem.* **2016**, *88*, 7206−7212 (ref 172). Copyright 2016 The American Chemical Society.

homeostasis is closely associated with some human diseases, such as cancer, neurodegenerative diseases, cardiovascular diseases, diabetes mellitus, and gastrointestinal diseases.[1−6] Therefore, cells possess an elaborate regulation system to maintain their redox balance and the large or significant redox state changes can be buffered by the redox-active molecules.[7,8] These molecules experience inter-reaction and interconversion to facilitate the dynamic balance of intracellular redox state, among which three types of representative molecules should be mentioned, including reactive oxygen species (ROS), reactive nitrogen species (RNS), and reactive sulfur species (RSS).

ROS are produced intracellularly through multiple mechanisms during the metabolism process. Also ROS mainly include superoxide anion ($O_2^{\bullet-}$), hydrogen peroxide (H_2O_2), singlet oxygen ($^1O_2$), hydroxyl radical ($^{\bullet}OH$), lipid peroxy radical ($ROO^{\bullet}$), ozone (O_3), hypochlorous acid/hypochlorite (HOCl/ClO^-), and hypobromous acid/hypobromite (HOBr/BrO^-).[9] Since the oxidation state of oxygen in ROS ranges from 2− to 0, ROS are highly reactive and are considered as one of the key

DOI: 10.1021/acs.analchem.7b04234
Anal. Chem. 2018, 90, 533−555

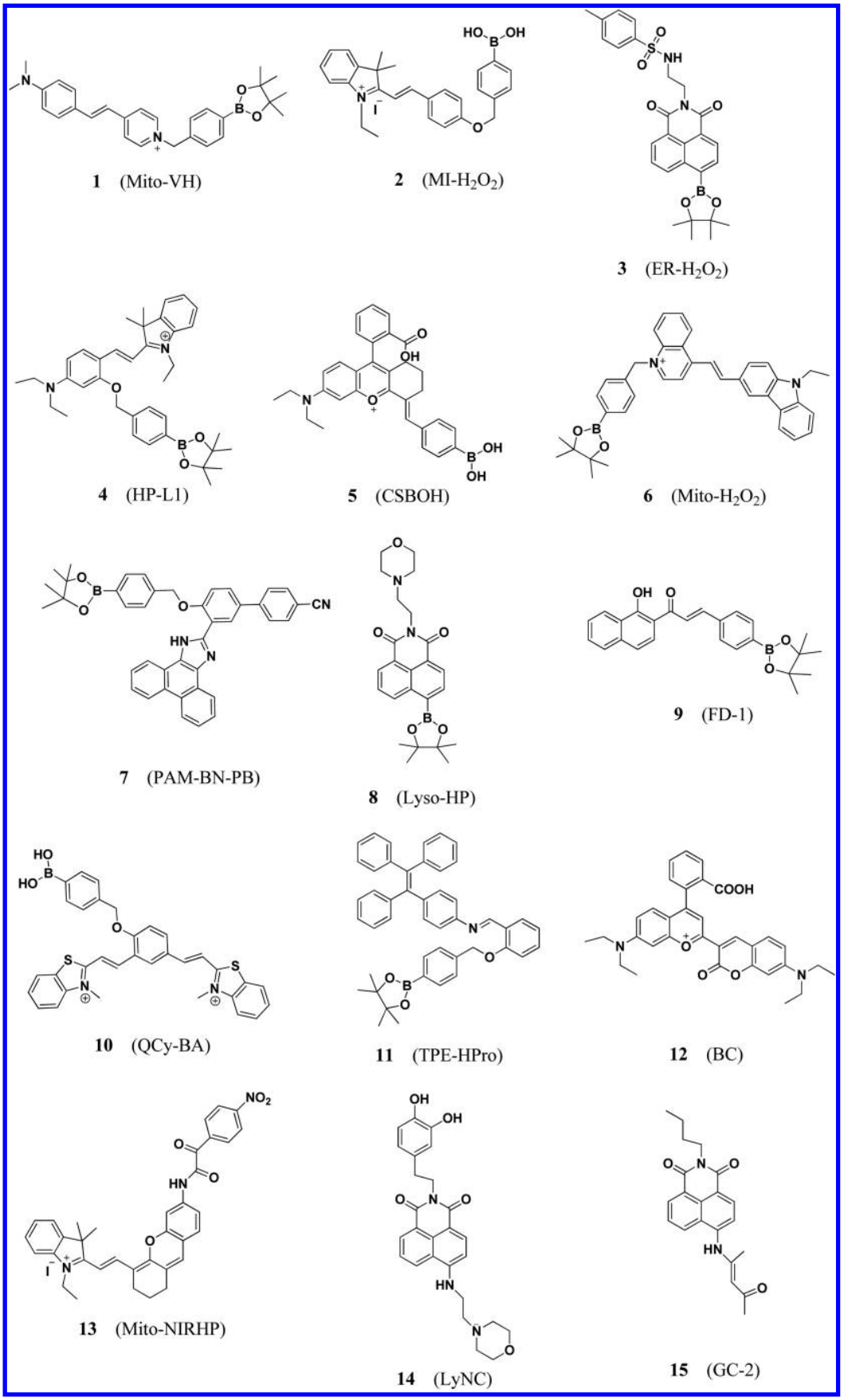

Figure 2. Structures of fluorescent probes for H_2O_2.

DOI: 10.1021/acs.analchem.7b04234
Anal. Chem. 2018, 90, 533−555

regulatory molecules for cells. ROS cannot only eliminate undesirable xenobiotics but also have great effects on cell signaling, which is vital for the regulation of physiological and pathological processes. RNS refer to NO and NO-related molecules with nitrogen oxidation state ranging from 1+ to 4+, such as peroxynitrite ($ONOO^-$), nitrogen dioxide (NO_2), S-nitrosothiols (RSNO), and nitroxyl (HNO).[10] RNS are able to react with a wide spectrum of biomolecules, including proteins, nucleic acid, and lipids, and may act as transporters of NO in the cell signaling events.[11,12] RSS is defined as "redox-active sulfur-containing molecules that are able, under physiological conditions, to either oxidize or reduce biomolecules".[13] RSS mainly include biothiols (GSH, Cys, Hcy), H_2S, thiyl radical ($RS^•$), disulfide (RSSR), sulfenic acid (RSOH), sulfur dioxide/sulfite/bisulfite ($SO_2/SO_3^{2-}/HSO_3^-$), persulfides (R−S−SH/H_2S_2), and polysulfides (R_2S_n/H_2S_n, $n > 2$). Sulfur in RSS possesses oxidation state ranging from 2− to 4+, endowing RSS with variable reactivity so that many redox reactions are mediated by RSS. In recent years, RSS biology has become an increasing focus of research.[13−16]

A growing body of research now shows that the multiple signaling transduction pathways are involved in the intracellular redox maintainance, which covers the active participation of ROS, RNS, and RSS (RONSS, for short).[14,17] The cross-talking between RONSS plays a very important role in the physiological and pathological processes.[14,17] The deep understanding or elucidation of the interaction among RONSS and its corresponding regulation effect on redox balance open up new area of research as well as new challenges in cell biology.

As the short lifetime, high reactivity, and transient conversion characters of RONSS, efficient analytical tool that can in situ monitor the generation, distribution, accumulation, and dynamic fluctuation of RONSS in biological systems can provide important information for their biofunction study. In recent years, because of the real-time, sensitive, and noninvasive characteristics, fluorescence imaging utilizing small-molecule fluorescent probes has become a powerful analytical tool to visualize the fluctuation and distribution of biomolecules.[18−20] Quite a number of fluorescent probes specific for RONSS have been designed and proposed based on different natures of RONSS, such as nucleophilic, electrophilic, oxidation, and reduction, etc (Figure 1).[16,18−20] Gratifyingly, some mechanisms and principles relating to the redox biochemistry have been revealed by these probes and researchers can understand more about the RONSS biofunctions than ever.

To display the recent progress in fluorescence imaging of RONSS, in this review, we aim to summarize the representative small-molecule fluorescent probes for RONSS in the last 2 years. The probes from our own group are also included. We mainly present the design, recognition, and response mechanisms of the probes. The probes which have not been applied in biological systems are not included.

FLUORESCENT PROBES FOR ROS

Fluorescent Probes for H_2O_2. H_2O_2 is one of the most important ROS, which is mainly generated from mitochondria by the activation of NADPH oxidase complex. As a second messenger, H_2O_2 is tightly linked to diverse cellular processes.[21−23] Whether it serves beneficial or harmful roles is closely associated with its distribution and concentration. In the last 2 years, a variety of fluorescent probes have been developed for detecting H_2O_2 in cells and animals. Collectively, four sensing strategies have been used, including the reaction of arylboronates or phenylboronic acid to phenols,[24−33] the conversion of oxonium or diketone to acid,[34,35] oxidation of phenol to quinone,[36] and carbon−carbon double bond cleavage.[37]

Probes Based on the Reaction of Arylboronates or Phenylboronic Acid to Phenols. The most commonly used sensing moiety for H_2O_2 is arylboronate, which has been accommodated in many fluorophores to obtain various probes. A mitochondria-targetable fluorescent probe **1** with two imaging channels for viscosity and H_2O_2 was proposed.[24] Besides the boronate for H_2O_2, the skeleton of **1** (Figure 2) is composed of N,N-dimethylamino as an electron donor, pyridinium cation as a mitochondrial targeting group and an electron acceptor, as well as double bond and benzene as the connector. Fluorescence imaging showed that **1** was highly selective and could monitor the level of H_2O_2 and viscosity changes in intracellular mitochondria.

To study the synergetic variation of H_2O_2 in different organelles, probes **2** and **3** (Figure 2) were developed for mitochondria and endoplasmic reticulum (ER) localization, respectively.[25] The merocyanine core of **2** and 1,8-naphthalimide fluorophore of **3** emit distinguishable fluorescence. By the dual-imaging of **2** and **3**, we can see that during mitochondria-oriented apoptosis, mitochondria H_2O_2 levels continuously increased first, whereas the ER H_2O_2 levels rose subsequently after a delay. However, during ER-oriented apoptosis, ER is the major site for overproduction of H_2O_2, and delayed elevation of the H_2O_2 levels was found in the mitochondria.

The pH-switchable fluorophores with different pK_a were used to construct probes for H_2O_2 that can be lighted on within certain acidity ranges. Probes **4**[26] and **5**[27] were developed for H_2O_2 under acidic and alkaline conditions, respectively. Probe **4** (Figure 2) possesses a spirobenzopyran fluorophore emitting strongly at lower pH, whereas **5** (Figure 2) has a Changsha near-infrared dye derivative giving ratiometric signal at higher pH. Both of these two probes showed high specificity to H_2O_2 and were used for live cell imaging. This type of probe provides a new strategy for the spatially confined imaging in certain cell regions.

Speed up the recognition reaction of arylboronates-based probes to H_2O_2 is vital since H_2O_2 is highly reactive and diffuses rapidly in cells. Therefore, several fast responsive probes were designed to improve the temporal resolution for H_2O_2 detection. *p*-Pinacolborylbenzyl was grafted on a quaternarized quinoline unit which was masked on a carbazole group to compose a fluorescent probe **6**[28] (Figure 2). Following the 1,6-rearrangement elimination by H_2O_2, the photoinduced electron transfer (PET) was inhibited and the fluorescence of **6** was turned on within 5 min. On the basis of a push−pull molecular frame and fluorescence turn on mechanism of ICT (intramolecular charge transfer), the Wang group[29] proposed a three-component fluorescent probe **7** (Figure 2) for H_2O_2 in Hela cells and *in vivo*. One highlight of **7** is its relatively short response time to H_2O_2 within 8 min because of the acceleration of nucleophilic reactions by benzonitrile. Another fast-responsive probe **8** was synthesized by Lin et al.[30] Probe **8** (Figure 2) has a simple structure with 1,8-naphthalimide fluorophore and lysosome-targeting morpholine moiety. Probe **8** exhibited a dynamic response of ∼2 min toward H_2O_2. The fourth H_2O_2-rapid-reaction probe **9** was based on a 4-hydroxybenzochalcone fluorophore.[31] Probe **9** (Figure 2) reacts with H_2O_2 in ∼3.5 min and can be used in tissue imaging.

The environmental sensitization for H_2O_2 detection was also performed. Environmental sensitization means that the fluorescence of the product of a H_2O_2-recognizable reaction

DOI: 10.1021/acs.analchem.7b04234
Anal. Chem. 2018, 90, 533−555

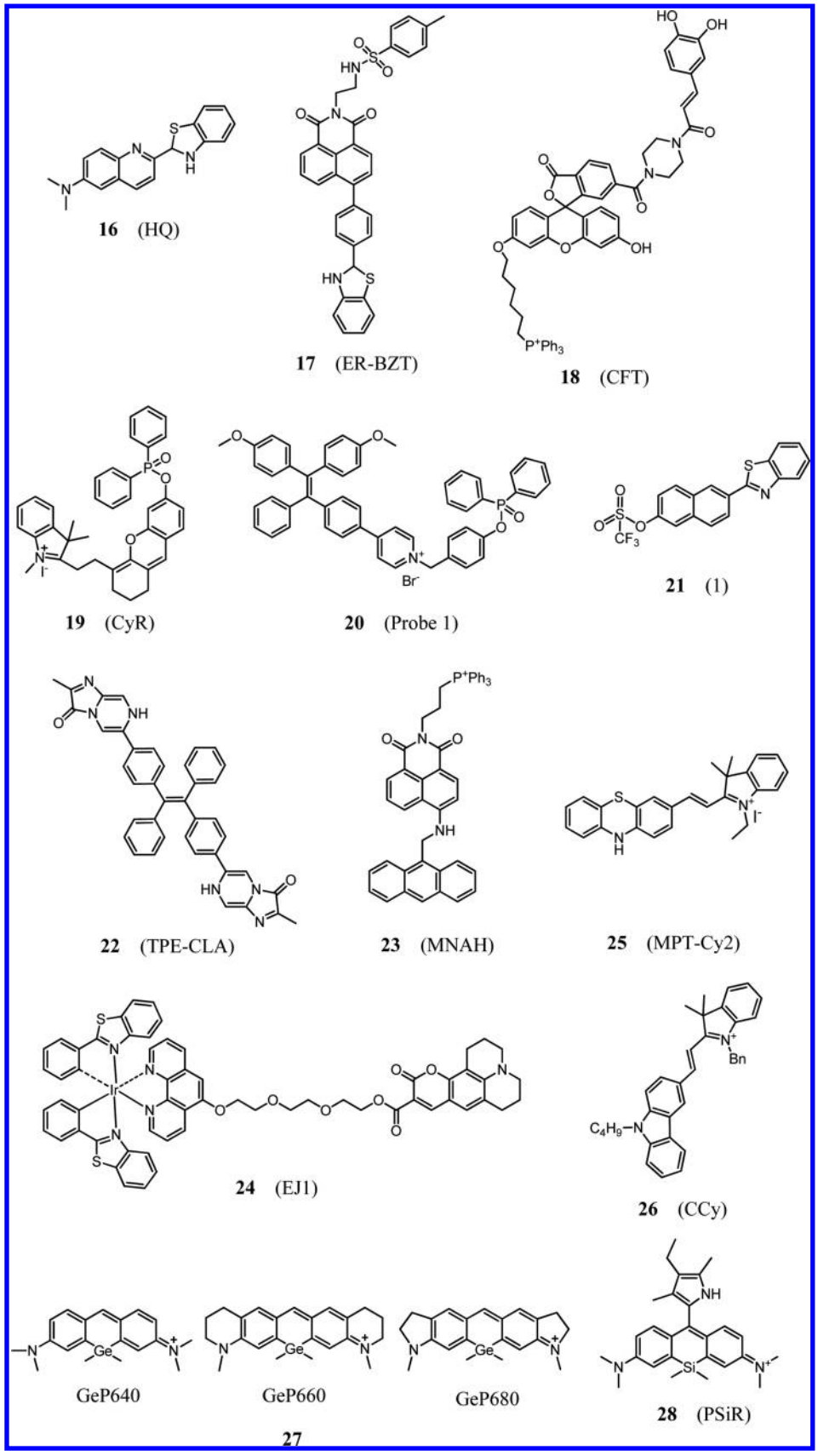

Figure 3. Structures of fluorescent probes for $O_2^{\bullet-}$, $^1O_2$, $^\bullet OH$, and total ROS.

can be dramatically enhanced in the presence of some specific environmental conditions or coexisting substances. A H_2O_2 specific and DNA-binding fluorescent probe **10** (Figure 2) was designed.[32] Reaction with H_2O_2 induces **10** to release a pro-fluorescent quinone-cyanine derivative with a one-donor-two-acceptor (D2A) structure which could switch-on NIR

DOI: 10.1021/acs.analchem.7b04234
Anal. Chem. 2018, 90, 533−555

fluorescence strongly through binding to the DNA minor groove. Bioimaging experiments demonstrated that probe **10** could detect and quantify H_2O_2 produced by EGF/Nox pathways and postgenotoxic stress in both primary and senescent cells. Probe **11** (Figure 2) derived from aggregation-induced emission (AIE) was proposed for H_2O_2 in the serum sample.[33] Probe **11** was integrated with tetraphenylethylene (TPE) as the core structure, the phenylboronic ester as the reaction site and the imine group as the emission mediator. The product from the reaction between **11** and H_2O_2 is polar sensitive and gives strong fluorescence in solution with water contents above 90%. Since H_2O_2 is quantitatively generated from the D-glucose−glucose oxidase system, **11** was utilized to monitor glucose concentration in buffer solution as well as in serum sample.

Probes Based on the Conversion of Oxonium or Diketone to Acid. On the basis of the Baeyer−Villiger oxidative rearrangement reaction, a NIR (near-infrared) fluorescent probe **12** (Figure 2) with an oxonium group in its benzopyrylium-coumarin skeleton was developed.[34] Oxonium can be nucleophilicly attacked by H_2O_2 to release the coumarin part, initiating a ratiometric response and large emission shift. Two-photon imaging by **12** realized the detection of exogenous and endogenous H_2O_2 in the living cells as well as in zebrafish.

α-Ketoamide moiety can be specificly switched to amine by H_2O_2 in aqueous solution. This reaction was utilized to design a new NIR fluorescent probe **13** (Figure 2), which was constructed by integrating α-ketoamide with hemicyanine fluorophore.[35] ICT mechanism was utilized to modulate the fluorescence change. It was proved that H_2O_2 is overgenerated during ischemia-reperfusion injury at both cell and organ levels by using **13**.

Probes Based on Oxidation of Phenol to Quinone. Probe **14** (Figure 2) with naphthalimide fluorophore and catechol sensing moiety was fabricated.[36] The oxidization of H_2O_2 converted the catechol into *o*-quinone, inhibiting the PET from the catechol moiety to the naphthalimide core to turn on fluorescence. Cell imaging confirmed that **14** could monitor endogenous H_2O_2 in lysosomes as well as in brain tissues and in living nematodes.

Probes Based on Carbon−Carbon Double Bond Cleavage. Utilizing the H_2O_2-promoted carbon−carbon double bond cleavage, probe **15** (Figure 2) with enamine group as the responsive moiety was fabricated.[37] Upon reaction with H_2O_2, a peroxide intermediate was formed, which then was transformed to stable amide, accompanying with blue fluorescence emission. Probe **15** was used to image H_2O_2 in cells, mouse liver slice, and tumor tissues.

Fluorescent Probes for $O_2^{\bullet-}$. $O_2^{\bullet-}$ is the "primary" ROS in living systems since it can be served as a precursor for many ROS, including H_2O_2, $^{\bullet}OH$, $^1O_2$, and ClO^-.[38] In addition, $O_2^{\bullet-}$ acts as a mediator in oxidative chain reactions.[39] Overproduction of $O_2^{\bullet-}$ initiates oxidative stress and disruption of the redox homeostasis. Normally, redox mechanism (oxidation ability of $O_2^{\bullet-}$) and nonredox mechanism (nucleophilicity or other reactive nature of $O_2^{\bullet-}$) are used to develop reaction-based fluorescence probes for $O_2^{\bullet-}$.

Probes Based on Redox Mechanism. Utilizing the oxidation properties of $O_2^{\bullet-}$, a two-photon fluorescent probe **16** for the detection and imaging of $O_2^{\bullet-}$ was developed (Figure 3). When the benzothiazoline group grafting onto quinoline scaffold was specifically dehydrogenized by $O_2^{\bullet-}$, fluorescence was turned on because of the extension of π-conjugations and the ICT process. Inspired by the satisfactory characteristics of **16**, in situ visualization of endogenous $O_2^{\bullet-}$ in lung inflammation samples was achieved.[40]

Using the same mechanism, another two-photon probe **17** (Figure 3), which was obtained by combining benzothiazoline to 1,8-naphthalimide with a endoplasmic reticulum-targeting benzsulfamide, was designed to image $O_2^{\bullet-}$ in diabetic mice.[41] Two-photon fluorescence imaging showed that the concentration of $O_2^{\bullet-}$ in abdominal or hepatic tissue of diabetic mice is higher than that in normal mice, and metformin pretreatment can depress $O_2^{\bullet-}$ level.

Probe **18** comprising covalently linked caffeoyl, fluorescein, and triphenylphosphonium (Figure 3) was developed for $O_2^{\bullet-}$ and pH in mitochondria.[42] Catechol moiety in caffeoyl could be readily oxidized by $O_2^{\bullet-}$ to *o*-quinone, giving fluorescence which is differential from fluorescein. With the assistance of **18**, it was found that inhibition of Dynamin-related protein 1 (Drp1) transduced a signal through mitochondrial complexes I and II to enhance the $O_2^{\bullet-}$ and pH levels. Eventually, mitohyperfusion and apoptosis in breast cancer cells happened.

Probes Based on Nonredox Mechanism. Several probes were constructed based on the nucleophilicity of $O_2^{\bullet-}$. Two probes of **19** and **20** (Figure 3) were developed through the nucleophilic and subsequent deprotection of the diphenyl phosphinate group by $O_2^{\bullet-}$. **19** is NIR-emissive and cell-membrane permeable, and was applied to image $O_2^{\bullet-}$ in zebrafish and mouse liver.[43] Probe **20** is a pyridine modified TPE compound with two-channel fluorescence. When the diphenyl phosphinate linked cresol-like structure was selectively fractured by $O_2^{\bullet-}$, the pyridine modified TPE was released. The original fluorescence emitted by donor−acceptor structure was lost and new aggregation emitted green fluorescence emerged. Intracellular $O_2^{\bullet-}$ fluctuation during apoptosis and inflammation was tracked and monitored by **20**.[44]

$O_2^{\bullet-}$ also can nucleophilicly attack trifluoromethanesulfonate group. Therefore, probe **21** (Figure 3) was proposed using a donor−acceptor (D−A) structured naphthalene derivative as a potent two-photon fluorophore.[45] The deprotection of trifluoromethanesulfonate by intracellular and tissue $O_2^{\bullet-}$ resulted in high fluorescence signal and deep imaging depth of ~150 μm.

A fluorescence/chemiluminescence dual sensing platform **22** (Figure 3) for $O_2^{\bullet-}$ was designed by covalently linking TPE and imidazopyrazinone moiety.[46] The reaction between $O_2^{\bullet-}$ and imidazopyrazinone induces apparent increase in both fluorescence and chemiluminescence. Besides the application in imaging $O_2^{\bullet-}$ in Raw264.7 cells and inflamed mice, acetaminophen induced $O_2^{\bullet-}$ in HL-7702 cells was uninterruptedly monitored by **22** with chemiluminescence and the results were further confirmed by fluorescence imaging.

Fluorescent Probes for $^1O_2$. $^1O_2$ is a highly reactive oxygen species (hROS) that oxidizes a broad range of biomolecules.[47,48] On the one hand, $^1O_2$ can facilitate the treatment of cancer by destroying tumor cells. On the other hand, $^1O_2$ can regulate the intracellular signaling pathways. As the short half-life ($\tau_{1/2} = 10^{-6} \sim 10^{-5}$ s) of $^1O_2$,[49] the fluorescence for $^1O_2$ needs a fast dynamic response.

The first two-photon fluorescent probe **23** (Figure 3) for imaging of $^1O_2$ in tissues was proposed by Zhang et al.[50] This mitochondrial-targeting probe **23** was designed based on the PET mechanism, integrating 9-methylanthracene, triphenylphosphonium, and naphthalimide core. When the 9-methylanthrance group acting as an electron acceptor trapped $^1O_2$ to inhibit the PET process, great fluorescence enhancement was observed. $^1O_2$ generation in mitochondria during the photodynamic therapy (PDT) was detected by **23**.

DOI: 10.1021/acs.analchem.7b04234
Anal. Chem. 2018, 90, 533−555

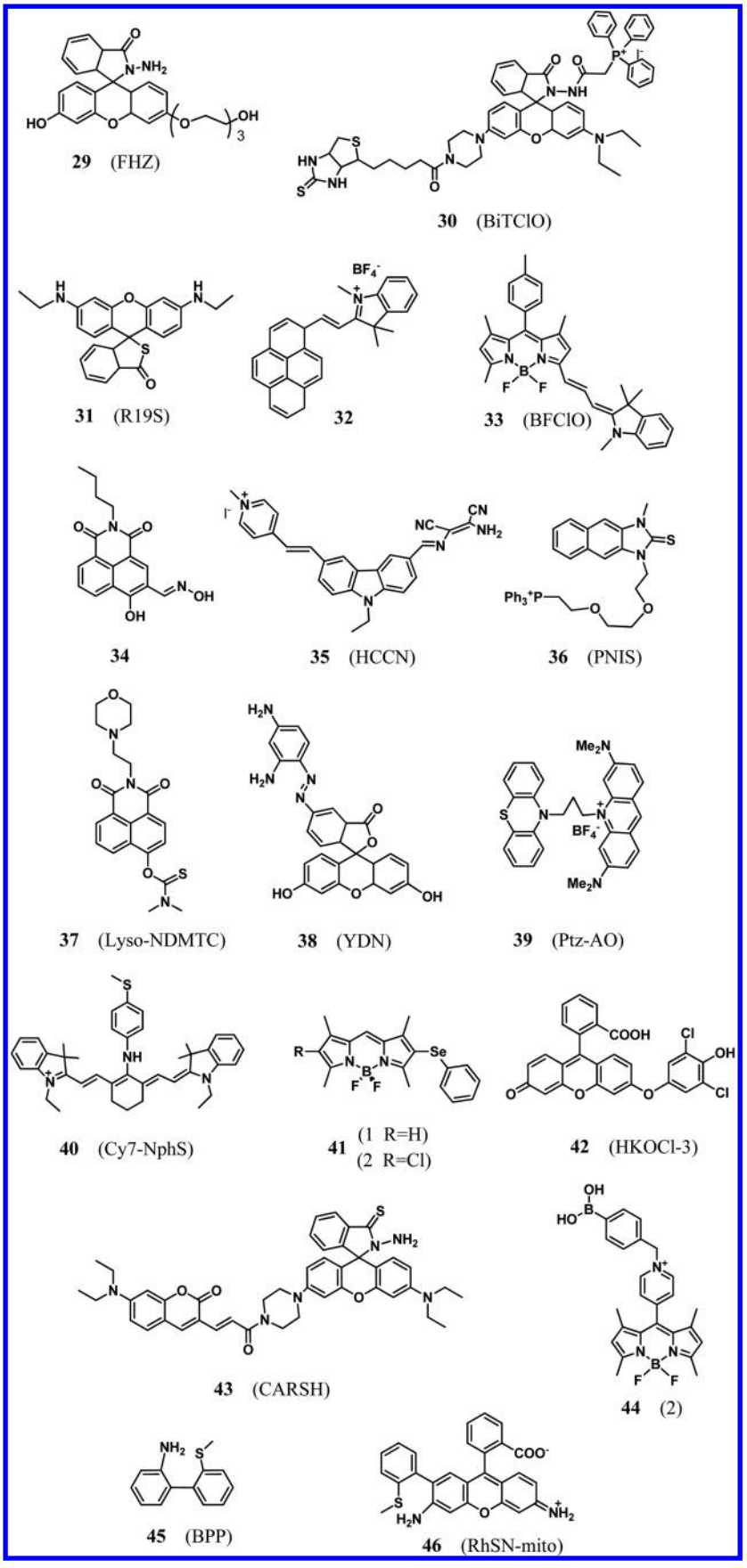

Figure 4. Structures of fluorescent probes for HClO/ClO$^-$ and HBrO/BrO$^-$.

DOI: 10.1021/acs.analchem.7b04234
Anal. Chem. 2018, 90, 533−555

A ratiometric photoluminescence probe **24** (Figure 3) was developed by connecting an Ir(III) complex and a coumarin 314 derivative.[51] The specific ratiometric signal was activated through the abstraction of the α-H from the tertiary amine by $^1O_2$. Probe **24** was used as a bioimaging agent to evaluate endogenously produced $^1O_2$ in cells.

Fluorescent Probes for $^{\bullet}$OH. As one of the most reactive and aggressive oxidizing agents, $^{\bullet}$OH plays important roles in immunity metabolism as well as in the environment.[52] The excessive production of $^{\bullet}$OH might cause serious damage to many biomolecules.[53,54] Fluorescent probes for $^{\bullet}$OH are exploited based on its oxidation ability.

Sulfur atom in phenothiazines conjugated with cyanine can be oxidized by $^{\bullet}$OH to yield sulfoxide. On the basis of this, a highly selective and mitochondria-targeting probe **25** was synthesized.[55] Probe **25** (Figure 3) showed a ratiometric variation in absorbance and dramatic enhancement in fluorescence. Interference of other hROS, including $ONOO^-$, ClO^-, and $^1O_2$ was negligible. Probe **25** was used to detect endougenous $^{\bullet}$OH in living cells and various type of bacteria. Finally, the toxicity of TiO_2NPs with different diameter was investigated in zebra fish embryos. The results showed that there was an inverse relationship between the TiO_2NPs diameter and their toxicity.

A fluorescent probe **26** (Figure 3) for the detection of $^{\bullet}$OH was designed based on hybride carbazole-cyanine dyes.[56] The oxidation of the pyrrolidine by $^{\bullet}$OH produced azole and turned on fluorescence. Probe **26** exhibited properties in terms of fast response, good selectivity, and low cytotoxicity. Probe **26** was successfully employed to monitor endogenous $^{\bullet}$OH in living HeLa cells.

Fluorescent Probes for Total ROS. A series of Ge-pyronine dyes (GePs, **27**) (Figure 3) were synthesized with emission wavelengths from deep-red to NIR. Replacing O with Ge increases $10^4 \sim 10^3$ times higher affinity toward GSH compared with the parent O-pyronine. Thus, GSH addition to 9-position C results in a quick quenching in 10 s and the fluorescence recovers in 20s by adding ROS. The redox switch can be repeated for several cycles. Probe **27** was used for real-time monitoring of the reversible and dynamic interconversion between ROS oxidation and GSH reduction in living cells.[57]

A lysosome-targetable NIR fluorescent probe **28** (Figure 3) for hROS was synthesized based on the Si-rhodamine skeleton.[58] When the pyrrole NH of **28** was oxidized by hROS to generate N-hydroxylation, the PET process was hindered to turn on the fluorescence. Probe **28** is resistant to autoxidation and photoxidation and responds to hROS quickly. Probe **28** was used to real-time and long-term image the basal or stimulated level of hROS in lysosomes. The results showed that the discrimination between normal cells and cancer cells as well as tumors and healthy tissues could be accomplished by **28**.

Fluorescent Probes for HClO/ClO^-. HClO/ClO^- is widely used as a disinfectant in daily life. Moreover, intracellular HClO is one of the hROS, which is generated by H_2O_2 and Cl^- catalyzed by myeloperoxidase (MPO).[59] During the process of aging and immune response, HClO has been proved to play an important role.[60] The significant oxidation ability of HClO, which comes from Cl atom of an oxidation state of 1+, builds the foundation of fluorescent probes for HClO. According to the reaction mechanism, we divided the probes into four categories, including oxidation cleavage of lactam or lactone,[61−63] oxidation cleavage of double bonds (C═C, C═S, C═N, and N═N),[64−70] oxidation of thioether or selenide,[71−73] and other oxidation-related mechanisms.[74−76]

Probes Based on Oxidation Cleavage of Lactam or Lactone. Probe **29** (Figure 4), a fluorescein-hydrazine derivative, was developed to detect HClO and $^{\bullet}$OH with different channels in biological systems.[61] The cleavage of lactam by HClO recovered the conjugated system of fluorescein and gives green emission. Living cell imaging demonstrated **29** could simultaneously monitor the endogenous HClO and $^{\bullet}$OH in zebrafish. Another lactam-cleavage probe was **30** (Figure 4),[62] which was a mitochondria targeting biotin−rhodamine−TPP conjugate. ClO^- interacted with benzoyl acetohydrazide moiety to bring out the spiroring-opening rhodamine within 10 s. Biotin moiety guarantees the tumor cell specificity.

A nonfluorescent probe **31** (Figure 4) was synthesized based on the ring masking by sulfur atom on rhodamine 6G. In the presence of HClO, thioester was broken and sulfur atom was replaced by an oxygen atom to recover highly fluorescent rhodamine.[63] Probe **31** could detect endogenous HClO in neutrophils in a mouse infection model and in drosophila.

Probes Based on Oxidation Cleavage of Double Bonds. A pyrene-based water-soluble fluorescent probe **32** (Figure 4) was synthesized.[64] When the C═C double bond connecting pyrene and merocyanine was broken by ClO^-, water-insoluble pyrenecarboxaldehyde was generated, leading to a ratiometric fluorescence signal. Endogenous HClO in RAW264.7 cells was detected by **32**. Another probe **33** with a C═C bond conjugated fisher aldehyde to BODIPY could also be broken by HClO. Probe **33** (Figure 4) was NIR emissive and lysosome targeting and demonstrated a fast response to HClO.[65]

Oxidative deoximation reaction was used to fabricate probes for HClO. Probe **34** (Figure 4) possesses a naphthalimide aldoxime core with large Stokes shift. HClO oxidatively removed the C═N bond, resulting in dramatic fluorescence enhancement.[66] As to probe **35** (Figure 4), the dediaminomaleonitrile reaction by ClO^- recovered the planarity of the molecule, changed the D−A structure, and finally increased the fluorescence intensity.[67]

The C═S bond was used as reactive site to design HClO-specific fluorescence probes. Taking advantages of imidazolium salts, a mitochondrial-targeting two-photon fluorescent probe **36** (Figure 4) was synthesized bearing imidazoline-2-thione to function as a ClO^- recognition unit. When the thione functional group was specially oxidized by ClO^-, the fluorescent imidazolium was produced. Probe **36** was soluble in pure aqueous solution and fluorescence produced by other ROS and RNS was negligible. Moreover, **36** was successfully applied to image ClO^- in Hela and HepG2 cells, and in astrocytes.[68] Based on the electrophilic addition of Cl^+ to the sulfur of a C═S bond, a probe **37** (Figure 4) for the picomolar level of native HClO in lysosome was synthesized.[69] **37** was successfully applied to discriminating tumor tissue from normal tissue in mice.

On the basis of the oxygenolysis of an azo moiety, probe **38** (Figure 4) for selective and sensitive detection of HClO over other ROS and RNS in absolute PBS solution was synthesized. An open-ring structure with green fluorescence was observed after the azo moiety was oxidatively cleaved. Fluorescence imaging in mouse supported the ability of **38** in biological applications.[70]

Probes Based on Oxidation of Thioether or Selenide. Through tethering acridine orange and phenothiazine with propane to generate PET process, a pH-independent probe **39** (Figure 4) was synthesized based on the HClO-promoted oxidation of phenothiazine to the phenothiazine sulfoxide and cation which prevented the PET pathway. Probe **39** showed high

DOI: 10.1021/acs.analchem.7b04234
Anal. Chem. 2018, 90, 533−555

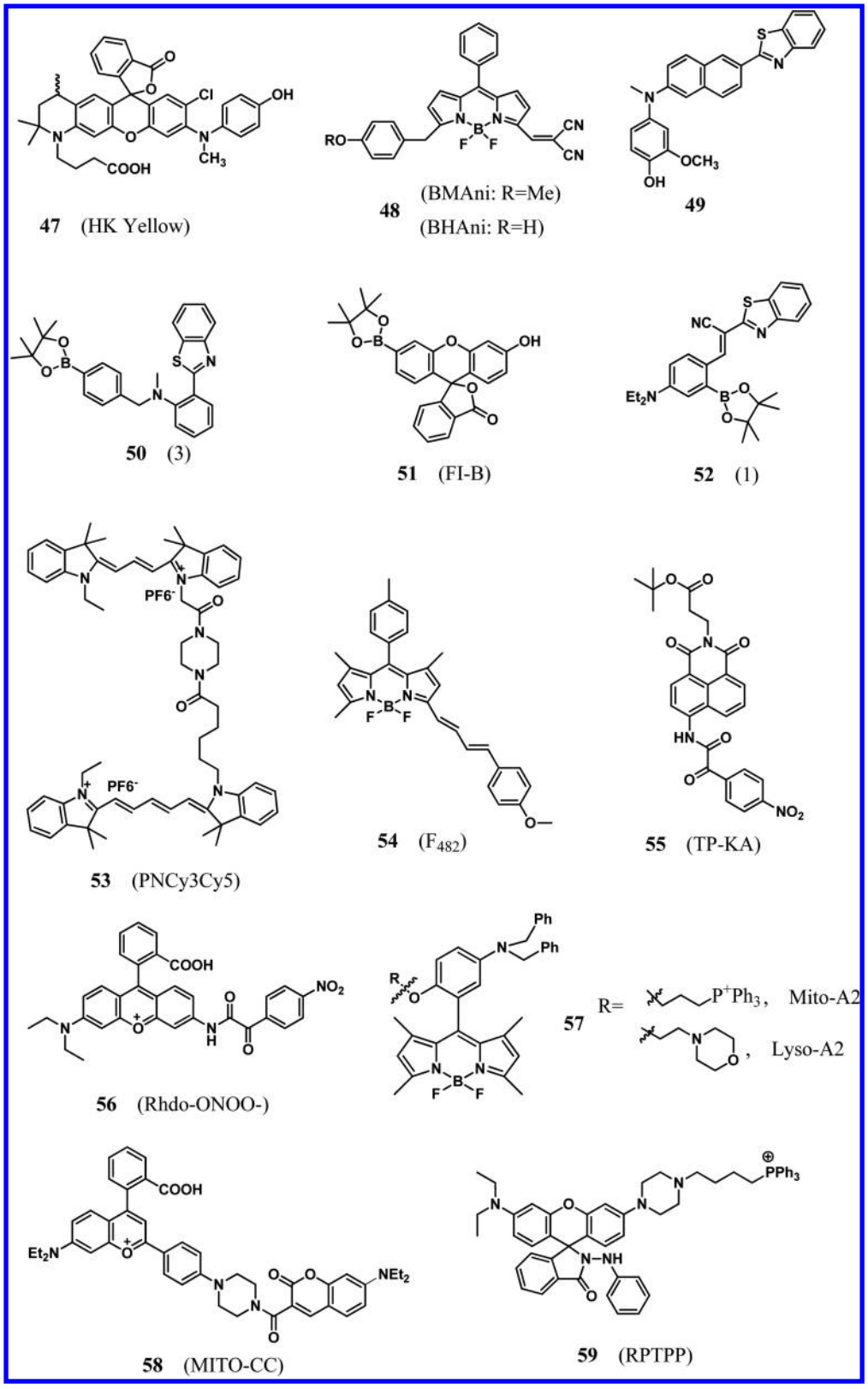

Figure 5. Structures of fluorescent probes for $ONOO^-$.

sensitivity (detection limit of 2.7 nM) and fast response (within 5 s) toward HClO in water. Probe **39** could efficiently detect HClO produced in stressed cells.[71] Another example was probe **40** (Figure 4) with a thioether-containing moiety that can be specificly oxidized into sulfoxide, which ruled out the fluorescence quenching through inhibiting the PET process.[72]

Two closely related phenyl selenyl based boron-dipyrromethene (BODIPY) turn-on fluorescent probes (**41**, Figure 4) for ClO^- were synthesized.[73] The probes showed high selectivity for ClO^-, and emission intensity reached a maximum within 1 s. When selenium was oxidized by HClO to selenoxide, the PET pathway was foreclosed which evoked a significant enhancement

DOI: 10.1021/acs.analchem.7b04234
Anal. Chem. 2018, 90, 533−555

in fluorescence. Living cell imaging studies showed that **41** possessed excellent cell membrane permeability and low cytotoxic properties.

Probes Based on Other Oxidation-Related Mechanisms. Since phenol can be oxidized to quinone and the incorporating ortho halogen substituents can improve the selectivity, a fluorescent probe **42** (Figure 4) for HClO was synthesized.[74] Oxidative O-dearylation of 2,6-dichlorophenol by HClO gave green fluorescence. Probe **42** exhibited high sensitivity (1 equiv of HOCl gave a >358-fold enhancement in fluorescence) and high selectivity (a >83-fold higher increase in fluorescence intensity over 1 equiv of $ONOO^-$ and $^{\bullet}OH$). Detection of endogenous HClO was operated in phagocytes as well as in living zebrafish embryos. Moreover, in flow cytometry and a 96-well microplate assay for the quantitative detection of endogenous HClO, **42** showed superior sensitivity.

A coumarin-alkene-rhodamin fluorescence resonance energy transfer (FRET) probe **43** (Figure 4) was designed with ratiometric signal for HClO.[75] The selective reaction between HClO and rhodamin thiohydrazide induced the dehydrogenation and spiro-ring opening, which realized the FRET process. Comparing to the traditional coumarin-rhodamin FRET platform, **43** exhibited high energy transfer efficiency (81.1%), making it suitable for detection in biological samples.

Phenylboronic acid group was found to be attacked and decomposed by ClO^-.[76] Probe **44** (Figure 4) consisting of meso-(4-pyridinyl)-substituted BODIPY as the chromophore group and phenylboronic acid as the sensing group was developed for ClO^-. Probe **44** was applied to imaging mitochondrial ClO^- in HepG2 cells.

Fluorescent Probes for HBrO/BrO^-. As an important ROS, HBrO generated from bromide plays a key role in the formation of sulfilimine cross-links in collagen IV.[77] Because of the approximately 1000-fold lower level of Br^- than that of Cl^-, the concentration of HBrO is relatively lower than that of HClO, making it difficult to detect. Only a small number of fluorescent probes were developed.

On the basis of the catalytic effect of HBrO on the cyclization between the amino group and S-methyl group, an ultrasensitive probe **45** (Figure 4) was developed for HBrO.[78] Probe **45** exhibits ultrasensitivity (down to 17 pM) and real-time response (within minutes) to HBrO. Endogenous HBrO in HepG2 cells and zebrafish was imaged by **45**. Utilizing the same mechanism, **46** (Figure 4) was designed for mitochondria HBrO.[79] Reaction with HBrO expanded the π-conjugation system of **46**, and NIR fluorescence was emitted, providing a tool for the study of physiological and pathological functions of HBrO.

FLUORESCENT PROBES FOR RNS

Fluorescent Probes for $ONOO^-$. Peroxynitrite ($ONOO^-$) is generated from radical coupling of nitric oxide (NO) and $O_2^{\bullet-}$ and can exert protective activity against invading pathogens or microbes.[80] As a highly potent oxidant, aberrant production of $ONOO^-$ can lead to oxidative damage which correlates with many pathological consequences, such as ischemia-reperfusion injury, cardiovascular diseases, neurodegenerative disorders, inflammation, and cancer.[81] For the past few years, considerable attention has been paid to the development of new fluorescent probes for the imaging of $ONOO^-$ in living systems. Collectively, there are mainly four strategies, including dearylation reaction to produce amido, deboronation, oxidation of unsaturated bond, and decomposition of α-ketoamide group, etc.

Probes Based on Dearylation to Produce Amido. $ONOO^-$ can trigger the N-dearylation reaction to remove the N-aryl. Rhodamine-based probe **47** (Figure 5) containing the N-aryl group as a fluorescence quencher and reaction site was constructed.[82] Probe **47** was water-soluble and virtually non-fluorescent. One equiv of $ONOO^-$ gave a 93-fold enhancement of fluorescence within 2 s while 1 equiv of $^{\bullet}OH$ or HClO did not interfere. Probe **47** was utilized to visualize endogenous $ONOO^-$ generated in mouse liver tissues under an acute alcohol binge condition and during hepatic ischemic-reperfusion injury. A similar fluorescent probe **48** (Figure 5) was designed based on the BODIPY scaffold masking with 4-hydroxyaniline, which was changed to 4-methoxyaniline in the presence of $ONOO^-$.[83] Probe **48** displayed high selectivity to $ONOO^-$ over other ROS (2 equiv of ROS did not elicit noticeable fluorescence changes). Another fluorescent probe **49** (Figure 5) utilizes benzothiazole as a two-photon fluorophore. Probe **49** presents a low detection limit (0.35 nM) and high specificity toward $ONOO^-$ and was used to image endogenous $ONOO^-$ in biological samples.[84]

Probes Based on Deboronation. Although arylboronate has been widely employed in the design of fluorescent probe for H_2O_2, in some cases it shows higher reaction rate with $ONOO^-$ than H_2O_2. This character was utilized in the development of $ONOO^-$ fluorescent probes.[85−87]

Fluorescent probe **50** (Figure 5) could be unmasked by $ONOO^-$ to release *N*-methyl-benzothiazole with the initiation of ESIPT, leading to fluorescence increase.[85] Since fluorescein is an easily detectable fluorescent compound with high quantum yield (Φ_{Fl} = 0.93−0.94), a fluorescein-boronate fluorescent probe **51** (Figure 5) was synthesized. The reaction rate of **51** with $ONOO^-$ was about 10^6 and 2700 times faster than that of H_2O_2 and HClO at 25 °C. The actual intracellular flux of $ONOO^-$ was estimated utilizing **51**.[86] In probe **52** (Figure 5), deboronation generated hydroxyl which intramolecularly cyclized to form a bright iminocourmarin fluorophore. The detection limit of **52** reaches 0.83 nM.[87]

Probes Based on the Breakage of Unsaturated Bond. The $ONOO^-$-induced diene oxidation has been utilized to design fluorescent probes.[88,89] Since Cy3 has a shorter polymethine chain and better stability to $ONOO^-$ than Cy5, a fine-tuning fluorescent probe **53** (Figure 5) was obtained through integrating Cy3 and Cy5 which usually act as a popular FRET pair. This mitochondria-targeting probe operates in a FRET-based ratiometric mode and the detection limit is 0.65 nM. Moreover, its applicability has been demonstrated for fluorescence imaging of $ONOO^-$ in stimulated macrophage cells.[88] Another specific probe **54** (Figure 5) was designed based on the BODIPY scaffold with trans-cinnamaldehyde molecules. It is ratiometric since the diene interconnection can be oxidized to form the BODIPY skeleton, accompanied by the fluorescence emission changes in the signal of red-to-green. High-throughput flow cytometry analysis indicated that **54** could quantify the $ONOO^-$ generation in the inflammation mouse model.[89]

Probes Based on the Decomposition of α-Ketoamide Group. Since $ONOO^-$ is a biomarker for certain drug-induced liver injury (DILI), two fluorescent probes were designed and applied to mapping $ONOO^-$ during DILI and the corresponding remediation pathway.[90,91] Probe **55** (Figure 5) could release 4-amino-1,8-naphthlic anhydride to restore ICT process and turn on fluorescence via the decomposition of α-ketoamide group. Probe **55** was used to evaluate the upregulation of $ONOO^-$ during acetaminophen (APAP) and tolcapone-induced hepatocyte injury. Another mitochondria-targeting probe **56** (Figure

DOI: 10.1021/acs.analchem.7b04234
Anal. Chem. 2018, 90, 533−555

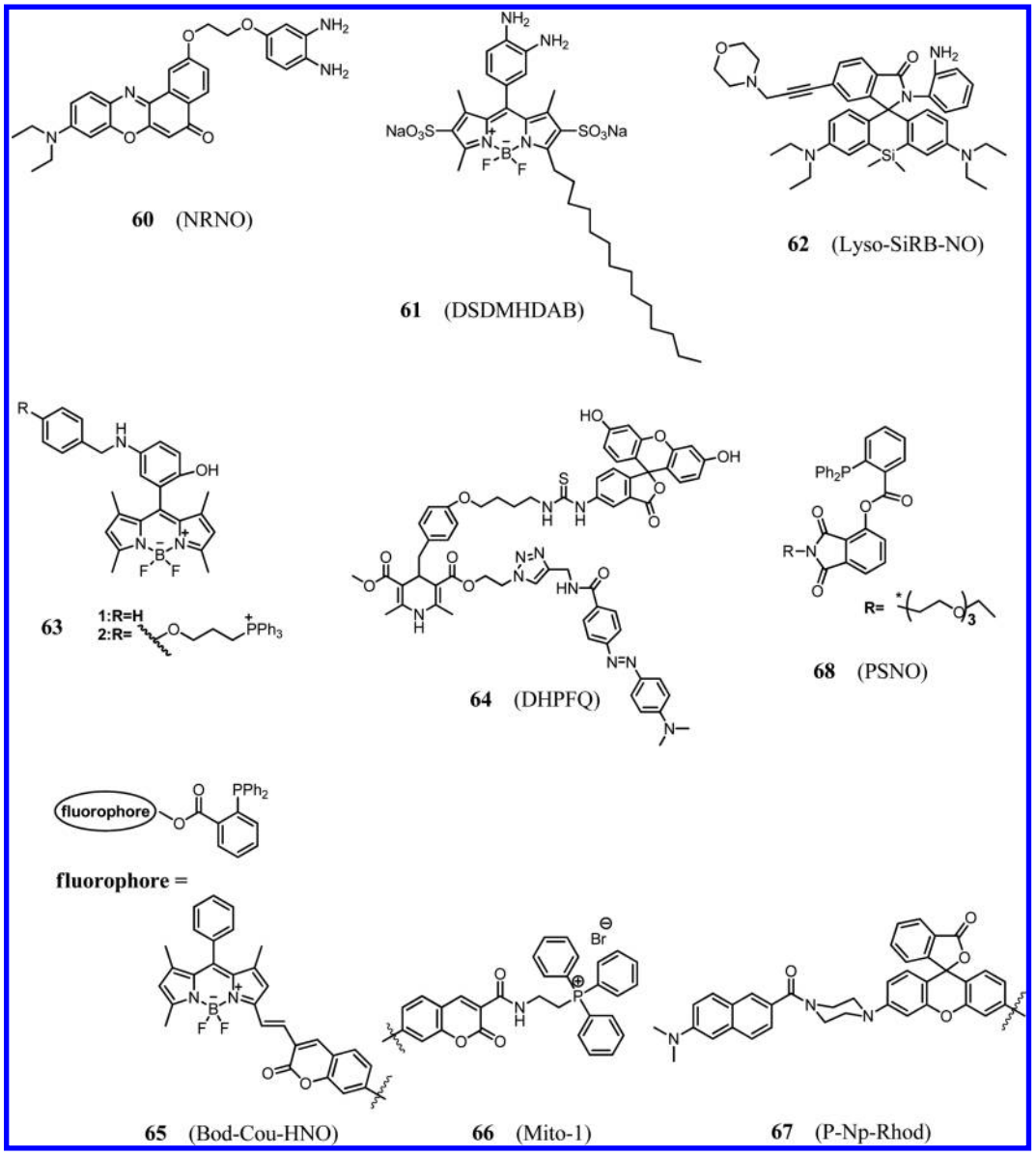

Figure 6. Structures of fluorescent probes for NO, HNO, and SNO.

5) with rhodamine skeleton revealed that CYP450/CYP2E1-mediated enzymatic metabolism of APAP leads to $ONOO^-$ generation in liver cells.[91]

Probes Based on Other Mechanisms. The $ONOO^-$-triggered N-oxidation and N-nitrosation reaction were utilized to design a new kind of fluorescent probe for $ONOO^-$. In probe **57** (Figure 5), BODIPY was installed with 4-methoxy substituted aromatic tertiary amine to quench fluorescence through the PET mechanism. When **57** was oxidized to produce N-oxide and N-nitroso products, the PET was blocked to recover fluorescence. Moreover, the mitochondria- and lysosome-targetable derivatives were used to image $ONOO^-$ in the corresponding subcellular organelles and in kidney tissues of diabetic rats.[92]

A two-photon ratiometric fluorescent probe **58** (Figure 5) for detecting mitochondrial $ONOO^-$ was designed based on the FRET mechanism.[93] Probe **58** combined a modified chromenylium fluorophore as the energy acceptor and the modified coumarin as the energy donor. Probe **58** is fast responsive (within 20 s) toward $ONOO^-$. Moreover, the minimal cytotoxicity of **58** enabled it to monitor endogenous $ONOO^-$ in both cells and LPS stimulated mouse model.

Mitochondria-targeting probe **59** (Figure 5) was installed by utilizing spirocyclic and nonfluorescent rhodamine as the fluorescence platform and phenylhydrazine as the recognition unit. The oxidative hydrolysis of phenylhydrazine by $ONOO^-$ could open the spirocyclic structure and turn on the fluorescence of rhodamine. Probe **59** is capable of monitoring the mitochondrial $ONOO^-$ level in live RAW 264.7 cells.[94]

Fluorescent Probes for NO. As a small uncharged free radical and ubiquitous messenger molecule, nitric oxide (NO) is implicated in many physiological and pathophysiological processes, such as endothelial dysfunction, cancer, and neurodegenerative diseases.[95−98] In recent years, the turn-on fluorescent probes for NO were mostly designed based on the inhibition of the PET pathway, including the reaction between NO and *o*-phenylenediamine to generate triazole[99−102] and N-nitrosation of aromatic secondary amine.[103,104]

Probes Based on the Formation of Triazole. As a two-photon fluorescent probe of NO, probe **60** (Figure 6) realized "NIR in"

DOI: 10.1021/acs.analchem.7b04234
Anal. Chem. 2018, 90, 533−555

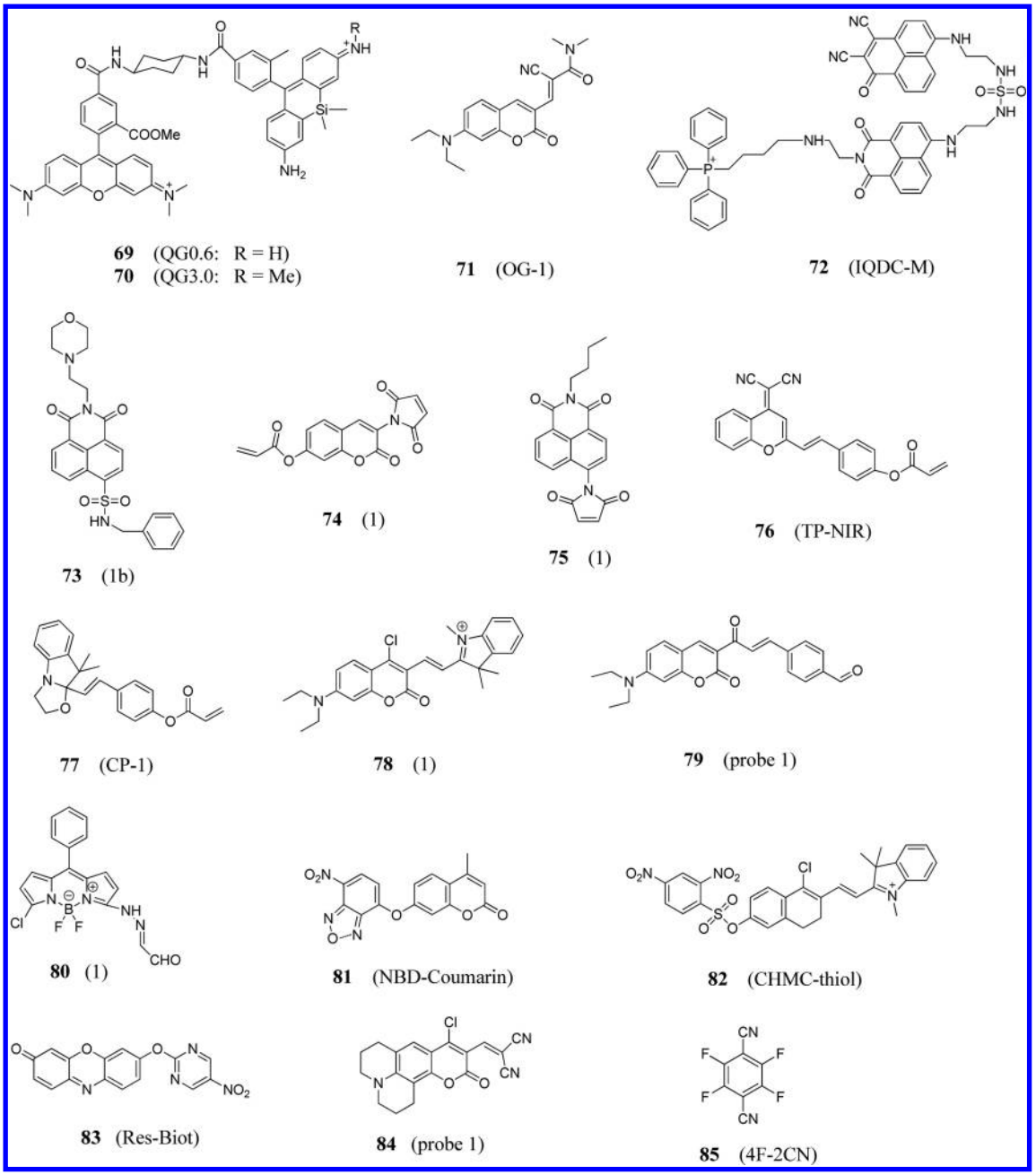

Figure 7. Structures of fluorescent probes for GSH, Cys, and Hcy.

and "far-red out" through utilizing Nile Red as the TP fluorophore and *o*-phenylenediamine as the reaction site. The reaction between **60** and NO could generate triazole which caused the inhibition of the PET process and enhancement of fluorescence. Compound **60** was utilized to measure both exogenous and endogenous NO in living cells as well as NO generation in LPS-mediated inflamed tissue of mice at depth up to 170 μm.[99]

Considering that most probes were developed for imaging intracellular NO and could not reflect the release and transmembrane behavior of NO, an amphiphilic probe **61** (Figure 6) containing hydrophilic groups to keep the fluorophore and recognition site outside the cell and an alkyl chain as the membrane anchor was designed based on BODIPY scaffold.[100] This highly water-soluble probe selectively monitored NO released out of the cells on the outer surface of RAW 264.7 murine macrophages and human vascular endothelial cells.

Probe **62** (Figure 6) was lysosome-targeting and was designed based on the *o*-phenylenediamine-locked Si-rhodamine skeleton.[101] This NIR fluorescent probe with a detection limit as low as 36.3 nM is stable in acidic solution and could monitor exogenous and endogenous NO in real time. Via change the Si-rhodamine lactam to deoxylactam, a probe with better properties was obtained which can avoid the serious interference from Cys. Moreover, this probe exhibits an ultralow detection limit (0.12 nM) and huge fluorescence off-on response (6300-fold).[102]

Probes Based on N-Nitrosation of Aromatic Secondary Amine. Mitochondria-targeting probe **63** (Figure 6) was designed based on the BODIPY dye masking with the *N*-benzyl-4-hydroxyaniline group which act as the reaction site for NO as well as the electron donor for PET, and triphenylphos-

DOI: 10.1021/acs.analchem.7b04234
Anal. Chem. 2018, 90, 533−555

phonium cation was introduced to act as the mitochondria-targeting group. Cellular experiments demonstrated that **63** was fast responsive (within seconds), highly sensitive (nannomolar level), and selective for NO over other various other ROS.[103] A similar probe was designed which consists of benzo[*g*]coumarin as the two-photon fluorophore. The probe could in situ monitor endogenous NO in live cells and in deep tissues. Moreover, this probe was utilized to monitor the NO generation in an ischemia reperfusion injury in the mouse model.[104]

Probes Based on Other Mechanisms. Since the C4-position of Hantzsch ester substituted with a benzyl group could react with NO to cleave the C−C bond, a novel FRET off-on NO fluorescent probe **64** (Figure 6) was designed. In this probe, 1,4-dihydro-pyridine acts as a linker to connect fluorescein isothiocyanate and [4′-(*N*,*N*′-dimethylamino)phenylazo] benzoyl as well as a quencher which could be released via the bond cleavage and recovered fluorescence. The specificity, sensitivity, and effectiveness of the reaction enabled the fluorescence intensity linearly with the amount of NO. On the basis of this, this ratiometric fluorescent probe semiquantitatively detected NO in the inflamed mice model.[105]

Fluorescent Probes for HNO. As a one-electron-reduced and protonated analogue of NO, nitroxyl (HNO) has been considered as a product of NO and H_2S in mammals.[106] Thus, the detection of HNO is really valuable to investigate the crosstalk between NO and H_2S in vivo.

Inspired by the specific reaction between HNO and phosphine, several fluorescent probes were designed.[106−109] The detection mechanism is the specific reaction between HNO and 2-(diphenylphosphino)-benzoate moiety and can give the corresponding aza-ylide, followed by the intramolecular attack to cleave the adjacent ester linker and released hydroxyl groups.

Probe **65** (Figure 6) was designed based on the BODIPY-coumarin conjugate platform. The reaction between HNO and the probe can produce the phenolate group which acts as a much stronger electron donor accompanied by the fluorescence enhancement at 463 nm and decreases at 592 nm. Furthermore, low cytotoxicity and good cell membrane permeability enabled **65** to be suitable for imaging of HNO in living cells.[107]

Probe **66** (Figure 6) was designed based on the coumarin core which endowed the two-photon property. The triphenylphosphine group was utilized as the mitochondria-targeting group and diphenylphosphine group as the reaction site. The detection limit of this mitochondria-targeting probe was as low as ∼18 nM which enabled one to detect the formation of exogenous and endogenous mitochondrial HNO.[108]

Since the FRET route can be switched off by the closed spirolactone form of the rhodol, a FRET-based two-photon ratiometric fluorescent probe **67** (Figure 6) was developed. The reaction between HNO and the probe could generate the fluorescent xanthene and induced the occurrence of FRET. This high selective probe could image HNO with dual-channel pattern in living cells and rat liver tissues with satisfactory deep-tissue imaging depth.[109] A similar ratiometric two-photon probe which contains benzo[*h*]chromene-rhdol skeleton was synthesized and successfully mapped the NO/H_2S cross-talk in vivo.[106]

Fluorescent Probes for SNO. Considering the crucial functional roles of S-nitrosylation in normal physiology and disease, a fluorogenic small molecular probe **68** (Figure 6) for the in situ imaging of GSNOs in live cells was designed. Since the 3-hydroxyphthalimide fluorophore was protected by 2-(diphenylphosphino) benzoic to block the ESIPT process, the probe was nonfluorescent. The reaction with GSNO could release the free phenol and turn on fluorescence. This probe exhibited good specificity toward GSNO which was chosen as a representative RSNO species. Because of the excellent biocompatibility, this turn-on fluorescent probe was successfully applied to image the dynamic change of protein S-nitrosylation in live endothelial cells.[110]

FLUORESCENT PROBES FOR RSS

Fluorescent Probes for GSH. Glutathione (GSH) is the most abundant (1−10 mM) and representative nonprotein thiol inside the cell which can be oxidized to its dimeric form, GSSG. GSH plays crucial roles in the intracellular antioxidant defense and associates with a wide variety of biological phenomena including inflammation, oxidative stress, gene expression, signal transduction, and apoptosis.[111] Therefore, the detection of GSH and its metabolism in biological samples is appealing. Generally, taking advantage of the nucleophilicity of GSH, the Michael addition reaction or the nucleophilic substitution was mainly employed to develop fluorescent probes for GSH tracing.

Probes Based on the Michael Addition. Inspired by extraordinarily fast reversible Michael addition−elimination reaction between silicon-substituted rhodamine, an electrophilic group, and the nucleophilic GSH, two reversible ratiometric fluorescent probes **69** and **70** (Figure 7) were designed to quantify intracellular GSH by utilizing a FRET platform. Tetramethylrhodamine (TMR), a typical rhodamine, was selected as an energy donor and silicon-substituted rhodamine was served as an energy acceptor.[112] After treated with GSH, the FRET process was interrupted due to the fluorescent quenching of acceptor. Meanwhile, the fluorescence of the response moiety was recovered when removing GSH, thus leading to a ratiometric readout. With high temporal resolution, these two probes were proved to be revolutionary tools to tracking and quantification GSH fluctuation under physical context. Another reversible ratiometric fluorescent probe **71** (Figure 7) was constructed to quantify GSH fluctuation in HeLa cells,[113] in which probe solution exhibited two different emission signals (λ_{Em}= 488 nm and λ_{Em} = 560 nm) that can be attributed to the change of the conjugated system after the Michael addition or elimination reaction between the probe and GSH.

On the basis of the Michael addition accompanied by the hydrolysis process, the fluorescent probes for GSH detecting were developed by integrating the alkene or alkyne group into an electron-withdrawing group carbonyl.[114,115] Upon incubation with GSH, the addition reaction performed first, and then the H-bond was formed between the N−H group of GSH and carbonyl to hydrolyze ultimately to a ring-opening compound with strong fluorescence, thus leading a fluorescent turn-on behavior.

Probes Based on the Nucleophilic Substitution. Utilizing nucleophilic substitution of GSH and proposed probes, a superior sulfonamide containing group was employed to constructed fluorescent probes with outstanding response behavior.[116−118] A FRET-based ratiometric fluorescent probe **72** was developed once sulfonamide group was introduced as a specific reaction site of GSH and the linker between the energy donor and acceptor.[117] Upon exposure to GSH, the S−N bond in the probes were cut off and the FRET pathway was interrupted resulting in ratio signals. In view of electron-withdrawing character of the sulfonamide group, the fluorescence of probe **73** was quenched on account of the inhibited ICT process once sulfonamide was integrated into naphthalimide.[118] The attack of GSH would locate GSH on the fluorophore and light up fluorescence through recovering ICT of naphthalimide.

DOI: 10.1021/acs.analchem.7b04234
Anal. Chem. 2018, 90, 533−555

Fluorescent Probes for Cys. As one of the sulfhydryl-containing small molecular amino acids, cysteine (Cys) plays crucial roles in many physiological and pathological processes. Excess amounts or deficiency of Cys are associated with diseases, while normal levels of Cys are essential for maintaining the synthesis of various proteins and act as the source of sulfide in human metabolism.[119,120] Therefore, the detection of Cys and its metabolism in biological samples is appealing. Overall, given the nucleophilicity of Cys, the Michael α,β-unsaturated addition reaction of Cys was a widely used design strategy to construct Cys specific probes.

Probes Based on the Addition of Maleimide. In view of extraordinarily fast reaction rates and outstanding specificity toward Cys residues in proteins, the maleimide group was integrated into well-known fluorescent reporters, such as coumarin[121] and naphthalimide,[122] to afford Cys specific fluorescent probes. Through combination of an acrylate group and a maleimide group onto the opposite sites of a coumarin fluorophore, a well-designed turn-on fluorescent probe **74** was obtained for Cys detection.[121] The two different recognition groups synergistically worked through different intramolecular cyclization processes. The thiol-Michael addition to the acrylate followed by the cyclization-deprotection step recovered its ICT process via changing the substituent from the electron-withdrawing ester to the electron-donating hydroxyl group, and the addition to the maleimide group removed its PET effect, ultimately resulting in the turn-on fluorescence response. Probe **74** could selectively detect and image Cys over Hcy and GSH in cells. The PET process caused by the response group maleimide endowed **75** with a low fluorescent background signal. Meanwhile, the strong electron-withdrawing ability of naphthalimide enhanced the reactivity of the probe which enabled the ultrasensitivity (2.0 nM). Moreover, this two-photon fluorescent probe could fast and selective image Cys in living cells.[122]

Probes Based on the Addition of Acrylate or Acrylate Derivatives. The acrylate or acrylate derivative was another wildly used trigger for constructing Cys specific fluorescent probes.[123−128] As a representative, a two-photon NIR turn-on fluorescent probe **76** was synthesized for specific detection of Cys over Hcy, GSH, and other amino acids.[123] The acrylate was masked on the dicyanomethylene-4H-pyran skeleton which has two-photon absorption. This probe has many excellent characters such as large Stokes shift (~150 nm), two-photon excitation (850 nm), and NIR emission (702 nm). All these enabled its application for biological imaging. A dual optical probe was reported based on the crotonyl group masking on the oxazolidinoindole-functionalized conjugated phenol.[125] After the Michael addition and a subsequent cyclization reaction of Cys, the fluorescence of the probe **77** was turned on as well as the solution color changed from colorless to red. Notably, the probe can be located in the mitochondria and can be attributed to the positive charge of the probe product.

Probes Based on the Addition of α,β-Unsaturated Ketone. Nucleophilic addition of Cys to the α,β-unsaturated ketone was employed to develop Cys fluorescent probes by integrating ketone to common dyes.[129−131] For example, a tailor-made specific fluorescent probe **78** was developed based on the 4-chlorocoumarin-hemicyanine framework to discriminate Cys from other thiols.[130] After incubation with Cys, the probe solution showed a maximal absorption peak blue-shift from 576 to 373 nm on account of the destruction of the conjugate structure that can be attributed to the substitution-rearrangement reaction of the primary amine of Cys, followed by the attack of liberated free thiol to the adjacent double bond, which is unavailable for other biothiols as well as NAC. Another representative α,β-unsaturated ketone containing fluorescent probe **79** was developed through incorporating the ethanoylcoumarin and terephthalaldehyde, in which the former acted as the Cys reaction site and the latter was a sensitive nucleophilic addition reaction site for SO_2.[131] Since SO_2 is the metabolite of Cys, this dual-site probe monitored the conversion of Cys and SO_2 in a ratiometric manner. Probe **79** also was the first probe to monitor endogenous SO_2 without stimulation of SO_2 donors. Bioimaging experiments demonstrated that **79** could quickly (within 100 s) and reversibly image Cys as well as SO_2 in two channels in A549 cells and zebrafish.

Probes Based on the Reduction of Aldehyde. Considering electron-withdrawing aldehyde could be reduced by Cys, a novel turn-on fluorescent probe **80** was designed for detection of Cys over Hcy/GSH as well as other amino acids.[132] The working mechanism of this BODIPY-based glyoxal hydrazone probe was the inhibited ICT quenching through addition to the unsaturated aldehyde, followed by the formation of a 5-membered ring of thiazolidine. Probe **80** was used to image intracellular Cys.

Fluorescent Probes for Hcy. The quite similar structure between Hcy and Cys makes the discrimination of Hcy over Cys a significant challenge. On the basis of 1,1′-binaphthyl fluorophore tethered to an aldehyde moiety, a Hcy specific fluorescent probe was designed through the cyclization reaction between Hcy and the aldehyde group in the probe. Once exposed to Hcy, a six-membered thiazinane was generated accompanying with fluorescence enhancement. ^{1}H NMR analysis was carried out to strongly verify the fluorescence increment triggered only by Hcy, rather than Cys, GSH, and other biothiols.[133]

Fluorescent Probes for Total GSH, Cys, and Hcy. *Probes Based on the Substitution of Benzoxadiazole.* A generic strategy for the detection and measurement of GSH in the absence and presence of Cys/Hcy was presented. In this strategy, a 7-nitro-2,1,3-benzoxadiazole (NBD) group was selected as the fluorescence-quenching group to conjugate with the fluorophore through sulfhydryl-labile ether linkage.[134,135] Probe **81** (Figure 7) is nonfluorescent due to ICT.[134] The substitution reaction of GSH to **81** resulted in one emission because of the release of the strong fluorescent fluorophore and nonfluorescent sulfur ether. Meanwhile, the substitution reaction of Cys/Hcy will exhibit two distinctly separated emissions since the cleavage product of Cys/Hcy will experience intramolecular Smiles rearrangement to form a new highly fluorescent compound, which is unavailable for the cleavage product of GSH. The two different emission spectra can be analyzed to detect and differentiate GSH from Cys/Hcy, facilitating detection of GSH both *in vitro* and *in vivo*.

Probes Based on the Substitution of 2,4-Dinitrobenzenesulfonyl. The electron-withdrawing 2,4-dinitrobenzenesulfonyl group was widely used as a trigger to assemble biological thiols specific fluorescent probes.[136−139] Biothiols could selectively induce the O−S bond to cleave and remove the 2,4-dinitrobenzenesulfonyl group which acted as a fluorescent quencher as well as response moiety. The release of the fluorophore resulted in a remarkable fluorescence light-up response. Notably, the concentration range-dependent fluorescent probe **82** for sensing of biological thiols was designed based on judicious selection of the corresponding sensitivity sites and the dye platform, which was hybrid from 7-hydroxycoumarin and merocyanine.[137] The 2,4-dinitrobenzenesulfonate moiety and the chloro group were chosen as the high- and low-sensitivity site of thiols, respectively. The removal of the 2,4-dinitrobenzene-

DOI: 10.1021/acs.analchem.7b04234
Anal. Chem. 2018, 90, 533−555

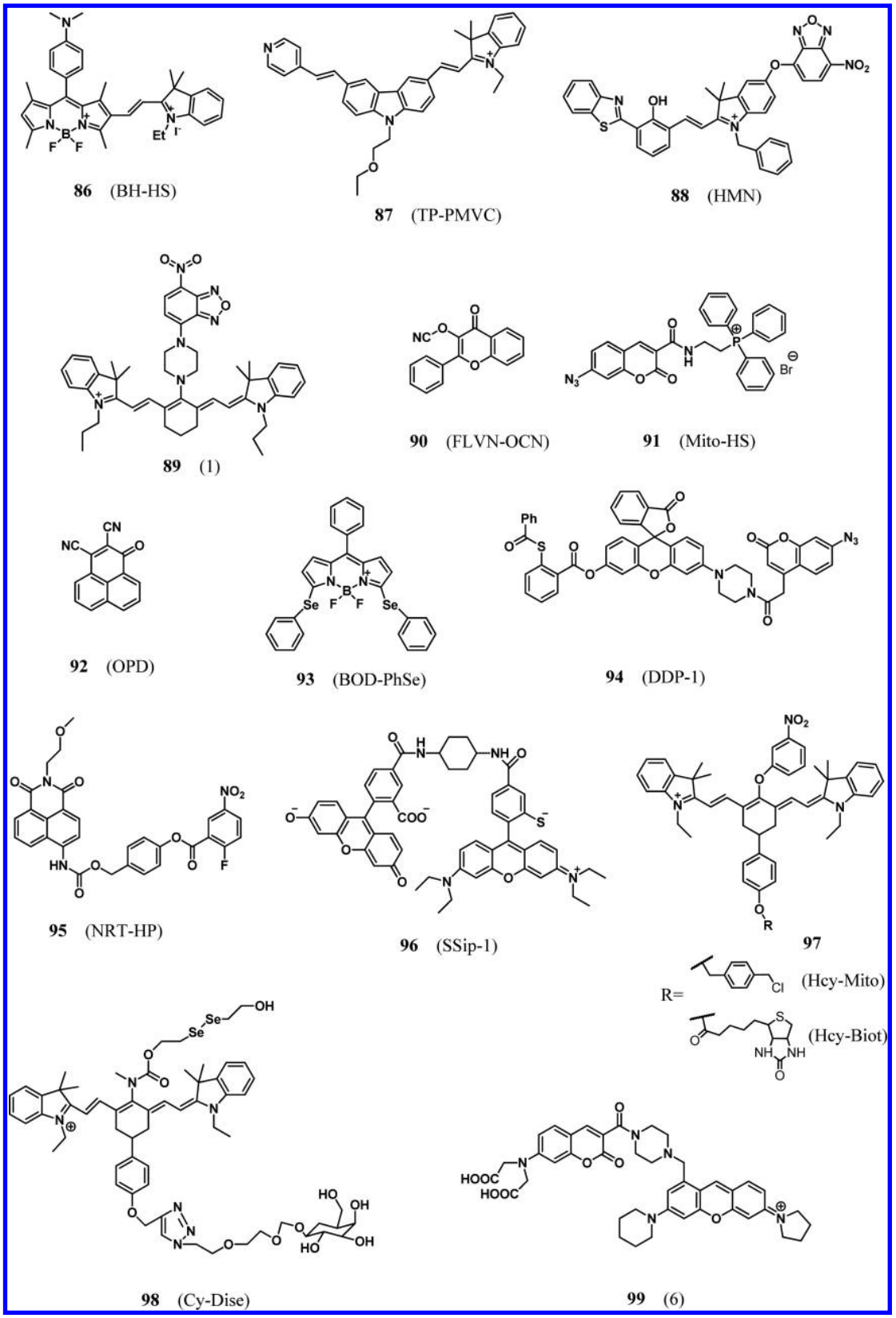

Figure 8. Structures of fluorescent probes for H_2S, H_2S_n, and Cys-SSH.

sulfontate moiety by the low concentration range (0−35 μM) of thiols exhibited a turn-on mode of fluorescence signal. Moreover, the 4-chloro group might be replaced by a high concentration range (35−500 μM) of thiols, followed by intramolecular S_NAr substitution to generate a 4-amino product and induce a ratiometric readout.

Probes Based on the Substitution of Pyrimidine. Grafting the pyrimidine group with different substituent on resorufin or fluorescein could obtain a series of fluorescent probe and

DOI: 10.1021/acs.analchem.7b04234
Anal. Chem. 2018, 90, 533−555

provided detailed structure−reactivity relationships.[140] Via this combinatorial strategy, fluorescent probe **83** for detection of biothiol was identified based on pyrimidine chemistry. It is the first time that the pyrimidine functionality was employed as the unique recognition unit to construct optical probe for biothiols. Probe **83** could be utilized as the analytical molecular tool in the living cell fluorescence imaging. Moreover, **83** could selectively visualize the endogenous biothiol fluctuations in mouse model.

Probes Based on the Addition of α,β-Unsaturated Malonitrile. By integrating α,β-unsaturated malonitrile and chlorine atom to the coumarin platform, a simple molecule probe **84** was developed.[141] The chlorine atom could be replaced by thiol group of biothiols and different products were produced through different cascade reaction, such as intramolecular rearrangement of the biothiols (Cys and Hcy) or cyclization reaction of the α,β-unsaturated malonitrile (GSH). Cell imaging studies indicated that **84** could simultaneously and selectively sense Cys and GSH in HeLa cells.

Probes Based on the Substitution of Tetrafluorotereph-thalonitrile. The currently smallest fluorescent probe **85**, which could differentiate Cys, Hcy and GSH was discovered.[142] The Cys thiol group replaced a fluorine on the probe and cyclized to form a six-membered ring with strong green fluorescence ($\lambda_{Ex/Em}$ at 420 nm/500 nm) and two-photon property (λ_{Ex}= 860 nm). The reactions between GSH/Hcy and **85** adopted aromatic nucleophilic substitution, generating products without two-photon property but with strong blue fluorescence ($\lambda_{Ex/Em}$ at 350 nm/450 nm). Addition of CTAB (cetyltrimethylammonium bromide) merely altered the fluorescence color of the reaction product of Hcy through facilitating the intramolecular ring formation ($\lambda_{Ex/Em}$ at 420 nm/500 nm). The results indicated the differentiation of these three thiols.

Fluorescent Probes for H_2S. As the smallest and simplest biothiol in living systems, hydrogen sulfide (H_2S) is known to be the third gaseous signal molecule following nitric oxide (NO) and carbon monoxide (CO).[143] Either protective or deleterious depending on its intracellular concentrations,[144] H_2S is supposed to influence various physiological and pathological processes, including the modulation of blood vessel tone and cardioprotection,[145] the endogenous stimulation of angiogenesis[146] and mitochondrial bioenergetics.[147] It has been reported that the physiological concentration of H_2S in mammalian serum is in the range of 30−100 μM, while those in the brain is in the range of 50−160 μM.[148] Considering the challenges in quantitatively detection of this volatile small molecule in living systems, the biologically relevant concentrations of H_2S may notably fluctuate with diverse types of cells and different subcellular regions. In view of the important roles of H_2S as a cytoprotectant and gasotransmitter, monitoring the level and dynamics of H_2S in living cells and organisms contributes to better understanding of its basic cellular functions. Based on the nucleophilic attack and reducing capacity of H_2S, strategies employed for the selective and sensitive detection of this small reactive molecule are classified into four categories in this review: nucleophilic addition, H_2S-induced thiolysis, azide group reduction and other novel recognition mechanisms.

Probes Based on Nucleophilic Addition of H_2S to Conjugated Systems. Given the nucleophilicity of HS^- at physiological pH, electrophilic centers in conjugated fluorescent molecules such as cyanine[149−152] or other dyes[153] can be feasibly attacked by H_2S-induced nucleophilic addition. Different signal transduction mechanisms including FRET,[149] TICT (twisted intramolecular charge transfer),[150] ICT,[151,152] and PET[152,153] were employed to develop fluorescent probes based on this reaction. Probe **86**,[150] as illustrated in Figure 8, was reported as the first TICT-based fluorescent probe for H_2S, using hemicyanine as recognition site for H_2S and BODIPY as the fluorescence reporting group. The nucleophilic addition of H_2S to the indole unit blocks the intramolecular TICT pathway and thus enhances the fluorescence. Notably, **86** specifically detected H_2S in a short response time (within 2 min for 50 μM H_2S), and visualization of exogenous as well as endogenous H_2S in living cells was achieved in this work. Carbazole platform was selected to develop a lysosome-targeting two-photon fluorescent probe **87** (Figure 8),[151] using pyridine moiety as the site for H^+ as well as the targeting group for lysosome and the indole unit as the reaction site of H_2S. Targeting to acidic lysosome exhibited a red-shifted fluorescence signal at 625 nm, while the nucleophilic addition of lysosomal H_2S to the indolenium C-2 atom produced a blue-shifted fluorescence readout at 550 nm. Accordingly, visualizing lysosomes and tracking lysosomal H_2S in living cells and mouse liver tissues, were achieved simultaneously with dual-channel fluorescent imaging in this work. The H_2S level in living systems is susceptible to levels of Cys, Hcy, and GSH, because of the close network of generation and metabolic pathways within biothiols. A hybrid multisignal fluorescent probe **88** (Figure 8),[152] was developed for simultaneously distinguishing and sequentially sensing Cys/Hcy, GSH, and H_2S for the first time. A red emission at 609 nm could be obtained upon the cut off of the ether bond by reaction with Cys/Hcy, GSH or low level H_2S, while another green emission at 546 nm was also observed for Cys/Hcy. Besides, high level H_2S generated a new blue emission at 485 nm. Accordingly, distinguishing fluorescence signals at three distinct emission bands (blue-green-red) with 61 and 63 nm interval distances between two adjacent bands, respectively, were collected upon responding to the respective biothiols. Three-color fluorescence imaging in living cells was acquired for simultaneous discrimination and sequential detection of Cys/Hcy, GSH and H_2S. Meanwhile, H_2S in a range of 0−0.5 mM could be detected in this work with changes of fluorescence at the blue and red emission bands.

Probes Based on H_2S-induced Thiolysis. Another nucleophilic attack strategy for H_2S-specific probes namely H_2S-induced thiolysis in this review, is based on the selective addition of HS^- to a single electrophilic position on the probe scaffold, which is followed by the removal of the electrophilic functionalities, resulting turn on fluorescent signals. The fluorescence of these probes are typically protected with incorporated electron withdrawing motifs that can be cleaved in the presence of H_2S. Thereinto, 7-nitro-1,2,3-benzoxadiazole (NBD) amine has been incorporated to naphthalimide,[154] styryl-BODIPY[155] and cyanine[156] skeleton to develop H_2S-specific fluorescent probes, based on their ability to undergo thiolysis by H_2S via a nucleophilic aromatic substitution (S_NAr) mechanism. A NIR fluorescent probe **89** (Figure 8),[156] based on the H_2S-thiolysis of NBD amine masking on the cyanine skeleton, was recently reported by Li group to explore its application in living mice. Endogenous H_2S in colorectal cancer cells in murine tumor model could be monitored *in situ* in living mice, through intratumoral injection of **89**. In addition to NBD, some electron withdrawing ester moieties[157−160] are also incorporated as leaving groups that could be specifically removed by nucleophilic H_2S to release fluorescent scaffolds with turn on signals. As illustrated in Figure 8, an electrophilic cyanate as the recognition site was masked on the 3-hydrozyflavone to develop an ESIPT-based fluorescent **90** (Figure 8)[158] for detection of H_2S in vitro

DOI: 10.1021/acs.analchem.7b04234
Anal. Chem. 2018, 90, 533−555

and imaging in living cells. Probe **90** was characteristic of high sensitivity with low detection limit (0.25 μM) and relatively quick response time (<60 s) toward H_2S over other biothiols.

Probes based on Azide Group Reduction. Electron-withdrawing azide moieties can be chemoselectively reduced to electron-donating amino products by H_2S, which are supposed to significantly change the electronic distribution of the whole molecule once installed onto fluorophores.[161−163] Probe **91** (Figure 8)[162] was reported to sense endogenous H_2S formation in cancer cells within 15 min without adding any external stimulators was reported recently, based on azide reduction. With the sensitivity of **91** toward H_2S as low as 24.3 nM, distinguishing cancer cells from normal cells was achieved based on the level of endogenous H_2S formation.

Probes Based on Other Reaction Mechanisms. Some novel reaction strategies for specific detection of H_2S have been investigated in the recent 2 years.[164−166] Nucleophilic aromatic substitution of hydrogen (S_NAr^H) reactions that can be catalyzed by sulfide, were employed to develop a phenalene-based fluorescent probe **92** (Figure 8)[164] for monitoring of aqueous sulfides in living cells. The mechanism was found to be that the sulfide added to the double bond, then underwent isomerization and rearrangement, followed by hydrolyzation and elimination to afford the final product. A fluorescent turn-off probe **93** (Figure 8)[166] was developed utilizing the phenylselenium group as a leaving group masking on the BODIPY core. Substitution of the phenylselenide group at the 3- and 5-position of BODIPY by H_2S accounted for the decrease in fluorescence intensity. Probe **93** was employed for imaging of intracellular H_2S in living cells in this work.

Fluorescent Probes for H_2S_n. With the in-depth understanding of physiological roles taken by RSS in cytobiology, increasing attention has been given to hydropersulfides (R-SSHs), which exhibit important biological activities in the modulation of enzyme functions and the synthesis of sulfur-containing vitamins and cofactors.[167] More recent studies on H_2S redox biology even suggest that R-SSHs account for most biological mechanisms which were originally attributed to H_2S.[167−169] H_2S_n can be considered as oxidized forms or redox partners of H_2S, which may coexist in biological systems as redox couple to collectively regulate sulfur-containing redox balance. As for the chemical reactivity, H_2S_n are expected to be stronger nucleophiles but weaker reductant than H_2S. To explore the varied roles of H_2S_n in biological systems, it is critical to employ effective analytical tool for detecting and monitoring the formation and consumption of these RSS species.

Phenyl 2-(benzoylthio)benzoate[170,171] and 2-fluoro-5-nitrobenzoic ester[172−174] are the two most used recognition units specific for H_2S_n. The first dual-channel fluorescent probe **94** (Figure 8)[170] capable of visualizing H_2S and H_2S_n with different fluorescence signals was developed in 2016, to reveal the mutual relationship and cross-talk between H_2S and H_2S_n in cells. Reaction with H_2S_n released the green fluorescence of rhodol at 542 nm, while recognizing H_2S produced the emission signals of both major blue coumarin major at 445 nm and minor green rhodol at 542 nm. Therefore, simultaneous appearance of the two well separated emissions confirmed the presence of H_2S, whereas single green emission was attributed to H_2S_n. Notably, **94** was successfully applied for the ratio detection ($F_{542\ nm}/F_{452\ nm}$) of relative H_2S_n and H_2S in mixture solutions with varying Na_2S_2/Na_2S concentrations. Bioimaging experiments proved that **94** could selectively detect H_2S and H_2S_n from distinct emission channels in HeLa cells. The first ratiometric fluorescent probe **95** (Figure 8)[172] for the detection of H_2S_n, was developed with 2-fluoro-5-nitrobenzoic group as a reaction unit. Via the formation of H_2S_n-mediated benzodithiolone, followed by the release of the electron-donating amino group to modulate the ICT system, **95** could image exogenous and endogenous H_2S_n in living cells.

Other reaction strategies can also be used to detect H_2S_n selectively. The unique reversible reaction of sulfane sulfur with other sulfur atoms was employed to develop a reversible fluorescent probe **96** (Figure 8)[175] for sulfane sulfur, based on FRET mechanism. The sulfur atom in SSip-1 could reversibly bind to sulfane sulfur, followed by the generation of intramolecular spirocylization of xanthene dye to turn on fluorescence. Concentration fluctuation of sulfane sulfur in living cells was reversibly visualized with **96** in this work. A multiresponse NIR fluorescent probe **97** (Figure 8)[176] for the *in situ* detection of endogenous $O_2^{\bullet-}$ and H_2S_n was designed based on heptamethine cyanine dye. The hydrogen in the probe could be extracted by $O_2^{\bullet-}$ to recover the conjugated system and emit low fluorescence. H_2S_n could revoke the PET process to provide stronger fluorescence through reducing the nitro group to amino group. Probe **97** could selectively image $O_2^{\bullet-}$ and H_2S_n in cells and in vivo.

Fluorescent Probes for Cys-SSH. Supposed to be the source of the whole profile of R-SSHs derivatives in living organisms at the micromolar level,[177] Cys-SSH is reported to play a leading role to synthesize sulfur-containing cofactors, regulate cellular signaling, modulate enzyme activities, and adjust cellular redox milieu.[167,178] The first near-infrared ratiometric fluorescent probe **98** (Figure 8)[179] for the detection of Cys-SSH in living cells and in vivo was developed in 2016, based on the selenium−sulfur exchange reaction. The diselenide group masking on the heptametine cyanine skeleton can be rapidly reduced by Cys-SSH within minutes, thus triggering the ICT process and exhibiting a larger spectral blue shift in emission from 797 to 749 nm. Quantitative detection of CBS enzyme-mediated Cys-SSH biosynthesis was achieved by ratiometric imaging analyses with fluorescence intensity ratio ($F_{749\ nm}/F_{797\ nm}$) in living cells. Meanwhile, **98** incorporated with liver-targeting galactose-terminated ligand was successfully applied to visualize Cys-SSH in peritoneal cavity of mice BALB/c and in hepatic carcinoma models. The first reversible ratiometric fluorescent probe **99** (Figure 8)[180] responsive to R-SSHs, including H_2S_2, Cys-SSH, and GSSH, was reported recently, based on the decrease of FRET efficiency after recognition. Once reversibly reacting with the pyronine fluorophore, the conjugated structure of the xanthene ring was interrupted and induced the dual-emission change at 479 and 584 nm. Probe **99** could dynamically visualize the concentration of R-SSHs in living cells by ratio imaging ($R = F_{430-480}/F_{550-630\ nm}$).

Fluorescent Probes for SO_2. Sulfur dioxide (SO_2) is widely present as an air pollutant in the environment which exists in the forms of sulfite (SO_3^{2-}) and bisulfite (HSO_3^-) anions in aqueous solution. Besides, SO_2 can be generated in the body during the oxidation of hydrogen sulfide or sulfur-containing amino acids metabolism. Recently, SO_2 is recognized as a gaseous signal transmitter modulating numerous biological processes. Abnormal levels of SO_2 and its derivatives (SO_3^{2-} and HSO_3^-) are closely associated with neurological disorders, cancers, and some other diseases.[181−184] Recently, there are some fluorescent probes reported for imaging SO_2 and its derivatives in living systems. Generally, these probes are mainly designed by exploiting the nucleophilic addition of SO_2 derivatives to the

DOI: 10.1021/acs.analchem.7b04234
Anal. Chem. 2018, 90, 533−555

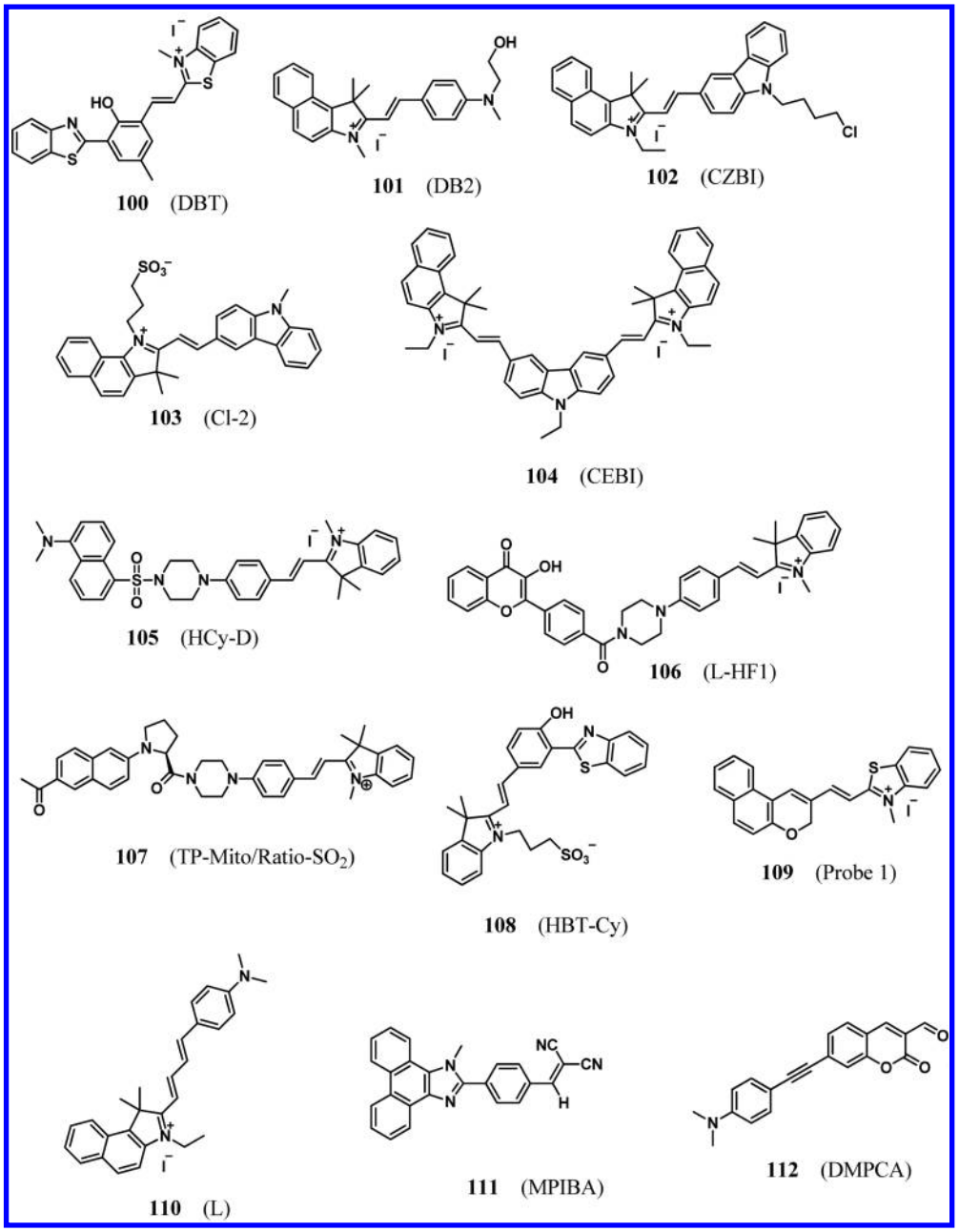

Figure 9. Structures of fluorescent probes for SO_2.

unsaturated bond. The α,β-unsaturated bond in the probe structure is easily attacked by the SO_2 derivatives to generate new blue-shifted fluorescence emission, thus resulting in the ratiometric fluorescence signal. The probes **100**−**104**[185−189] (Figure 9) are designed by applying this strategy. The alternative strategy of designing ratiometric fluorescence probes for SO_2 is modulating the FRET process. The probes **105**−**107**[190−192] (Figure 9) present the emission of the FRET acceptor whose conjugation structure is easily disturbed by nucleophilic addition of SO_2 derivatives to quench the fluorescence emission. Therefore, upon reaction with SO_2, the fluorescence switch to blue-shifted emission which attributes to the FRET donor, giving the ratiometric fluorescence signal for SO_2 quantification.

A new ratiometric fluorescent probe **108** (Figure 9) was proposed for reversible detection of HSO_3^- by conjugating benzothiazole and functionalized cyanine dye.[193] Nucleophilic addition of HSO_3^- to the probe resulted in distinct ratiometric fluorescence response, and subsequent treatment of the addition product by peroxides would restore the original probe in high yield. Fluorescence imaging experiments indicated that this probe could sense HSO_3^- reversibly in living cells as well as in aqueous solution. Besides, another fluorescent probe **109** (Figure 9) was developed by conjugating naphthopyran and benzothiazolium to reversibly image bisulfate/H_2O_2 redox cycle in live cells and zebrafish.[194]

Probe **110** (Figure 9) was designed to detect SO_3^{2-} and SO_4^{2-}/HSO_4^- simultaneously.[195] The probe itself was non-fluorescent. Upon treatment with SO_3^{2-}, the addition of SO_3^{2-} to the probe structure could restrict the ICT pathway due to the disruption of the conjugation and result in the fluorescence turn-on response at 442 nm. Besides, the presence of SO_4^{2-}/HSO_4^- induced the aggregation-induced emission to enable the turn-on fluorescence response at 511 nm. Fluorescence microscopic images indicated that this probe could differentially sense

DOI: 10.1021/acs.analchem.7b04234
Anal. Chem. 2018, 90, 533−555

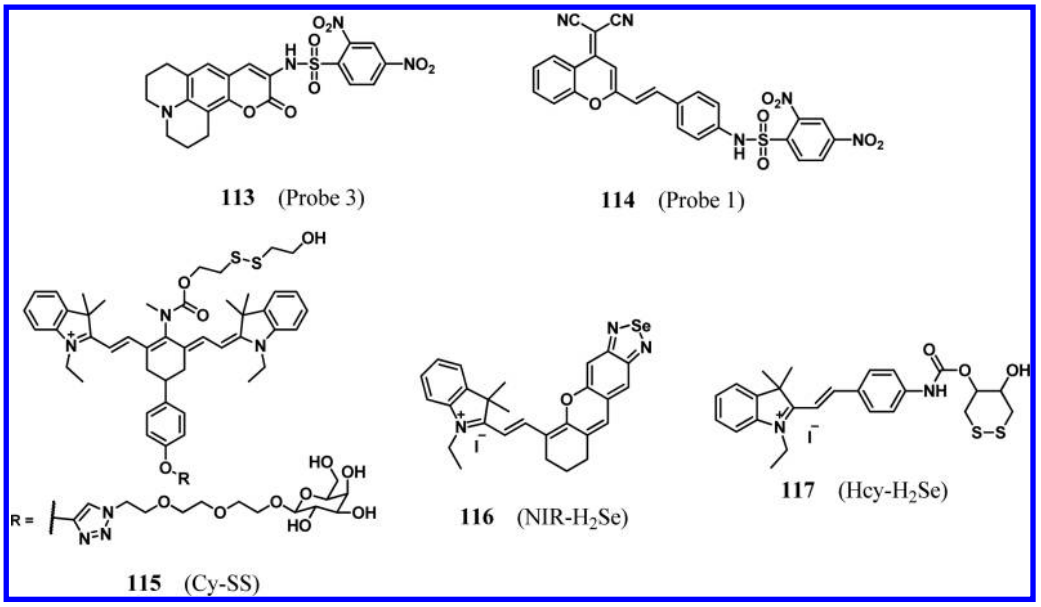

Figure 10. Structures of fluorescent probes for Sec and H_2Se.

intracellular SO_3^{2-} and SO_4^{2-} inside live HeLa cells. Probe **111** (Figure 9) was designed to detect SO_2 and ClO^- simultaneously.[196] This probe consisted of a phenanthroimidazole-modified fluorophore and a benzylidene malononitrile moiety as the reaction site of ClO^- and SO_2. Nucleophilic addition of SO_2 to this probe resulted in fluorescence emission at 410 nm within 60 s, while oxidation of ClO^- to this probe resulted in fluorescence emission at 500 nm within seconds. The probe was applied in detecting SO_2 and endogenous ClO^- in cells as well as visualizing the homeostasis of SO_2/ClO^- in zebrafish, which confirmed the oxidative-and-antioxidative effects of intracellular SO_2.

By exploiting aldehyde functionality as the reaction site for nucleophilic addition of HSO_3^-, probe **112** (Figure 9) was developed based on the coumarin skeleton through modulating the TICT process.[197] Additionally, the N,N-dimethyl group was selected as the TICT donor and the phenyl alkynyl was introduced to improve two-photon fluorescence characteristic. This probe successfully detected HSO_3^- in Hela cells under two-photon excitation.

Fluorescent Probes for Sec and H_2Se. Besides reactive sulfur species (RSS), reactive selenium species are other intracellular antioxidant systems, mainly including selenocysteine (Sec) and hydrogen selenide (H_2Se). Sec, the counterpart of cysteine, is the essential building block of selenoproteins which are involved in various biological processes and associated with cancers, inflammations, neurodegenerative disorders, and other significant diseases. H_2Se, the counterpart of H_2S, is considered an important metabolite of selenium-containing compounds. Similarly, endogenous H_2Se has been found to modulate various pathophysiological phenomena and associated with significant diseases.[198−202] Therefore, as a chalcogen like sulfur, selenium endows reactive selenium species reaction activities similar to RSS and fluorescent probes of Sec and H_2Se may greatly contribute to the deep understanding of their biological functions.

Probes **113** and **114** (Figure 10) are designed by integrating the 2,4-dinitrobenzenesulfonamide moiety to a certain fluorophore, which can be attacked by Sec to release the fluorophore and restore the fluorescence emission. Probe **113**[203] is based on the aminocoumarin platform, which exhibits near-zero background fluorescence as well as high specificity for Sec over competing amino acids and biothiols. Fluorescence imaging experiments indicated that this probe could monitor endogenous Sec in human cancer cells and zebrafish. Probe **114**[204] is developed based on the NIR fluorophore, dicyanomethylene-benzopyran. This probe was applied to image Sec in serum samples, live cells, and animals.

Probe **115** (Figure 10) was designed for Sec sensing by exploiting the selenium−sulfur exchange reaction.[205] This probe consists of heptamethine cyanine as NIR fluorophore, bis(2-hydroxyethyl) disulfde as the recognition unit, and D-galactose as the liver targeting moiety. The probe was used to evaluate the antioxidant and anti-inflammatory effect of Sec during liver inflammation. By comparing Sec levels in normal and acute hepatitis mice models, Sec was proved to be critical to maintain the redox states of the liver.

Probe **116** (Figure 10) was designed to detect H_2Se based on the NIR merocyanine dye core.[206] H_2Se can easily break the Se−N bond in the 2,1,3-benzoselenadiazole moiety via nucleophilic addition to generate diamino merocyanine fluorophore and restore the fluorescence emission. This probe is used to image endogenous H_2Se in live cells and in vivo with high selectivity over H_2S, Sec, and biological thiols. With the help of this probe, it is indicated that the anticancer mechanism of Na_2SeO_3 under a hypoxic environment is not a ROS-induced apotosis pathway but a nonoxidative stress mechanism. Probe **117** (Figure 10) was constructed by integrating the 1,2-dithiane-4,5-diol recognition unit onto the hemicyanine dye via an ester linker.[207] Since the disulfide bond in a six-membered ring is more stable than that in the chain structure, this probe can specifically detect H_2Se over thiols, H_2S, and Sec. H_2Se cleaves the disulfide bond, followed by the intramolecular cyclization to release the fluorophore and restore the fluorescence. It is demonstrated that this probe could sensitively monitor H_2Se in live cells and in vivo. Moreover, the generation and accumulation of H_2Se in HepG2 cells under hypoxic conditions and in the solid tumor were also revealed with the aid of this probe.

DOI: 10.1021/acs.analchem.7b04234
Anal. Chem. 2018, 90, 533−555

CONCLUDING REMARKS

In this review, we summarized the small-molecule fluorescent probes for imaging and detection of reactive oxygen, nitrogen, and sulfur species (RONSS) that developed since 2016. The probes consisted of various fluorophores and recognition moieties, providing an effective tool box for RONSS detection in living organisms. Undoubtedly, the further exploration of RONSS biology will be readily pushed forward by these new probes. Meanwhile, some issues need further thinking. Since the same recognition moiety accommodated to different fluorophores will exhibit specificity to different targets, the structure−reactivity relationships of the reported probes need deep investigation to draw the inherent rules, which can guide the purposeful design and synthesis of probes. Although the detection of endogenous analytes in vivo is generally accessed, the imaging depth is still limited because of low light penetration ability and stability of the probes. NIR and two-photon probes with low background interference help solve part of this but not all of it. The significant improvements may be afforded by using NIR-II window (1000−1700 nm)-emissive probes, which is characteristic of good imaging resolution and depth. The research progress in this area should be paid attention.[208] In some cases, influence of the cellular microenvironment on probe response characteristics cannot be neglected. The preliminary experiment in cell extracts or simulated cell physiological conditions may contribute to the identification of the difference, guiding the observation in living cells or in vivo. Finally, considering the short lifetime and high reactivity of RONSS, the concentration driven reversible probes with an ideal dissociation constant (K_d) that can real-time quantitative monitoring of RONSS are still highly needed, in spite of such probes being proposed for GSH.[112,113,209,210] Collectively, these issues provide not only a challenge but an entry to a new area of study for researchers. We believe that, with the development of new small-molecule fluorescent probes, the physiological and pathological functions of RONSS in biological systems will be better interpreted and understood.

AUTHOR INFORMATION

Corresponding Authors

*Fax: +86-531-86180017. E-mail: tangb@sdnu.edu.cn.

*E-mail: wangxu@sdnu.edu.cn.

ORCID

Bo Tang: 0000-0002-8712-7025

Notes

The authors declare no competing financial interest.

Biographies

Xiaoyun Jiao received her B.S. (2000) and M.S. (2003) degrees from Shandong Normal University (SDNU) and her Ph.D. (2007) degree in Organic Chemistry from Nankai University. She is now a lecturer of College of Chemistry, Chemical Engineering and Materials Science at Shandong Normal University. Her research interests are focused on the design and synthesis of new fluorescent probes for biological applications.

Yong Li was born in Hubei, China, 1990. He got his B.S. in Chemistry from SDNU in 2013. Currently, Li is pursuing his Ph.D. at the same school under the supervision of Prof. Bo Tang, focusing on the development of organic fluorescent probes for biological molecules to investigate their physiological and pathological functions.

Jinye Niu got her Master's degree under the mentorship of Bo Tang at SDNU, where she carried out research on the analytical applications of water-soluble CdTe-based fluorescent nanowires for detecting Cu^{2+}, avidin, and DNA in solutions at physiological pH. Niu is currently pursuing her Ph.D. in the same group, focusing on the development of fluorescence-based multimodal probes for sensing reactive small molecules in living systems.

Xilei Xie received his B.S. in pharmacy from Shandong University in 2008 and his Ph.D. in medicinal chemistry from the Institute of Materia Medica, Chinese Academy of Medical Sciences and Peking Union Medical College in 2014. Currently, he is a lecturer at SDNU. His research interests focus on the design and synthesis of novel functionalized probes for biological application.

Xu Wang received his Ph.D. in Environmental Sciences from the Research Center for Eco-Environmental Sciences, Chinese Academy of Sciences in 2006. From 2006 to 2008, he conducted postdoctoral research at the Department of Chemistry, Tsinghua University. He is now a Professor of Analytical Chemistry at SDNU. His current research interests are focused on the development of luminescent probes for biological applications.

Bo Tang is a Professor of Chemistry at SDNU. He received his Ph.D. (1994) from Nankai University. He began his independent career as a Professor of Chemistry at SDNU in 1994. In 2007, he was granted the National Science Fund for Distinguished Young Scholars in China. His research interests include the development of functional molecular probes and nanomaterials for biochemical analysis, clean synthesis of chemicals, and exploring new technology for solar energy chemical transformation and storage. He has contributed more than 300 journal articles as well as 21 invited book chapters and reviews and obtained 39 granted patents.

ACKNOWLEDGMENTS

This work was supported by the National Natural Science Foundation of China (Grants 21535004, 21390411, 21775093, 21375080, and 21505088).

REFERENCES

(1) McBean, G. J.; Aslan, M.; Griffiths, H. R.; Torrão, R. C. *Redox Biol.* **2015**, *5*, 186−194.

(2) Blázovics, A.; Kovacs, A.; Szilvás, A. *Acta Biologica. Szegediensis* **2009**, *53*, 3−6.

(3) Circu, M. L.; Aw, T. Y. *Free Radical Biol. Med.* **2010**, *48*, 749−762.

(4) Ueda, S.; Masutani, H.; Nakamura, H.; Tanaka, T.; Ueno, M.; Yodoi, J. *Antioxid. Redox Signaling* **2002**, *4*, 405−414.

(5) Powis, G.; Gasdaska, J. R.; Baker, A. *Adv. Pharmacol.* **1996**, *38*, 329−359.

(6) Afanas'ev, I. *Oxid. Med. Cell. Longevity* **2010**, *3*, 361−373.

(7) Valko, M.; Leibfritz, D.; Moncol, J.; Cronin, M. T. D.; Mazur, M.; Telser, J. *Int. J. Biochem. Cell Biol.* **2007**, *39*, 44−84.

(8) Nordberg, J.; Arner, E. S. *Free Radical Biol. Med.* **2001**, *31*, 1287−1312.

(9) Lou, Z.; Li, P.; Han, K. *Acc. Chem. Res.* **2015**, *48*, 1358−1368.

(10) Procházková, D.; Wilhelmová, N.; Pavlík, M. Reactive Nitrogen Species and Nitric Oxide. In *Nitric Oxide Action in Abiotic Stress Responses in Plants*; Khan, M., Mobin, M., Mohammad, F., Corpas, F., Eds.; Springer: Cham, Switzerland, 2015.

(11) Radi, R. *J. Biol. Chem.* **2013**, *288*, 26464−26472.

(12) Gordge, M. P.; Xiao, F. *Br. J. Pharmacol.* **2010**, *159*, 1572−1580.

(13) Gruhlke, M. C. H.; Slusarenko, A. J. *Plant Physiol. Biochem.* **2012**, *59*, 98−107.

(14) Winyard, P. G; Rrent, B.; Eggleton, P.; Nissim, A.; Taylor, E.; Lo Faro, M. L.; Burkholz, T.; Katalin, E.; Taylor, S.; Fox, B.; Viner, N.; Haigh, R. C.; Nigel, B.; Jones, A. M.; Whiteman, M. *Biochem. Soc. Trans.* **2011**, *39*, 1226−1232.

(15) Giles, G. I.; Tasker, K. M.; Jacob, C. *Free Radical Biol. Med.* **2001**, *31*, 1279−1283.

DOI: 10.1021/acs.analchem.7b04234
Anal. Chem. 2018, 90, 533−555

(16) Lin, V. S.; Chen, W.; Xian, M.; Chang, C. J. *Chem. Soc. Rev.* **2015**, *44*, 4596−4618.
(17) Mishanina, T. V.; Libiad, M.; Banerjee, R. *Nat. Chem. Biol.* **2015**, *11*, 457−464.
(18) Yuan, L.; Lin, W.; Zheng, K.; He, L.; Huang, W. *Chem. Soc. Rev.* **2013**, *42*, 622−661.
(19) Li, X.; Gao, X.; Shi, W.; Ma, H. *Chem. Rev.* **2014**, *114*, 590−659.
(20) Chan, J.; Dodani, S. C.; Chang, C. J. *Nat. Chem.* **2012**, *4*, 973−984.
(21) Kamata, H.; Honda, S.; Maeda, S.; Chang, L.; Hirata, H.; Karin, M. *Cell* **2005**, *120*, 649−661.
(22) Finkel, T.; Holbrook, N. J. *Nature* **2000**, *408*, 239−247.
(23) Winterbourn, C. C. *Nat. Chem. Biol.* **2008**, *4*, 278−286.
(24) Ren, M.; Deng, B.; Zhou, K.; Kong, X.; Wang, J.-Y.; Lin, W. *Anal. Chem.* **2017**, *89*, 552−555.
(25) Xiao, H.; Li, P.; Hu, X.; Shi, X.; Zhang, W.; Tang, B. *Chem. Sci.* **2016**, *7*, 6153−6159.
(26) Liu, J.; Ren, J.; Bao, X.; Gao, W.; Wu, C.; Zhao, Y. *Anal. Chem.* **2016**, *88*, 5865−5870.
(27) Liu, K.; Shang, H.; Kong, X.; Ren, M.; Wang, J.; Liu, Y.; Lin, W. *Biomaterials* **2016**, *100*, 162−171.
(28) Xu, J.; Zhang, Y.; Yu, H.; Gao, X.; Shao, S. *Anal. Chem.* **2016**, *88*, 1455−1461.
(29) Chen, Y.; Shi, X.; Lu, Z.; Wang, X.; Wang, Z. *Anal. Chem.* **2017**, *89*, 5278−5284.
(30) Ren, M.; Deng, B.; Wang, J.-Y.; Kong, X.; Liu, Z.-R.; Zhou, K.; He, L.; Lin, W. *Biosens. Bioelectron.* **2016**, *79*, 237−243.
(31) Huang, J.; Li, T.; Liu, R.; Zhang, R.; Wang, Q.; Li, N.; Gu, Y.; Wang, P. *Sens. Actuators, B* **2017**, *248*, 257−264.
(32) Narayanaswamy, N.; Narra, S.; Nair, R. R.; Saini, D. K.; Kondaiah, P.; Govindaraju, T. *Chem. Sci.* **2016**, *7*, 2832−2841.
(33) Song, Z.; Kwok, R. T. K.; Ding, D.; Nie, H.; Lam, J. W. Y.; Liuc, B.; Tang, B. Z. *Chem. Commun.* **2016**, *52*, 10076−10079.
(34) Dong, B.; Song, X.; Kong, X.; Wang, C.; Tang, Y.; Liu, Y.; Lin, W. *Adv. Mater.* **2016**, *28*, 8755−8759.
(35) Xie, X.; Yang, X.; Wu, T.; Li, Y.; Li, M.; Tan, Q.; Wang, X.; Tang, B. *Anal. Chem.* **2016**, *88*, 8019−8025.
(36) Reja, S. I.; Gupta, M.; Gupta, N.; Bhalla, V.; Ohri, P.; Kaur, G.; Kumar, M. *Chem. Commun.* **2017**, *53*, 3701−3704.
(37) Li, N.; Huang, J.; Wang, Q.; Gu, Y.; Wang, P. *Sens. Actuators, B* **2018**, *254*, 411−416.
(38) Turrens, J. F. *J. Physiol.* **2003**, *552*, 335−344.
(39) Sheng, Y.; Abreu, I. A.; Cabelli, D. E.; Maroney, M. J.; Miller, A. F.; Teixeira, M.; Valentine, J. S. *Chem. Rev.* **2014**, *114*, 3854−3918.
(40) Li, R.-Q.; Mao, Z.-Q.; Rong, L.; Wu, N.; Lei, Q.; Zhu, J.-Y.; Zhuang, L.; Zhang, X.-Z.; Liu, Z.-H. *Biosens. Bioelectron.* **2017**, *87*, 73−80.
(41) Xiao, H.; Liu, X.; Wu, C.; Wu, Y.; Li, P.; Guo, X.; Tang, B. *Biosens. Bioelectron.* **2017**, *91*, 449−455.
(42) Zhang, W.; Wang, X.; Li, P.; Xiao, H.; Zhang, W.; Wang, H.; Tang, B. *Anal. Chem.* **2017**, *89*, 6840−6845.
(43) Zhang, J.; Li, C.; Zhang, R.; Zhang, F.; Liu, W.; Liu, X.; Leeb, S. M. Y.; Zhang, H. *Chem. Commun.* **2016**, *52*, 2679−2682.
(44) Gao, X.; Feng, G.; Manghnani, P. N.; Hu, F.; Jiang, N.; Liu, J.; Liu, B.; Sun, J.; Tang, B. *Chem. Commun.* **2017**, *53*, 1653−1656.
(45) Lu, D.; Zhou, L.; Wang, R.; Zhang, X.-B.; He, L.; Zhang, J.; Hu, X.; Tan, W. *Sens. Actuators, B* **2017**, *250*, 259−266.
(46) Niu, J.; Fan, J.; Wang, X.; Xiao, Y.; Xie, X.; Jiao, X.; Sun, C.; Tang, B. *Anal. Chem.* **2017**, *89*, 7210−7215.
(47) Wilkinson, F.; Helman, W. P.; Ross, A. B. *J. Phys. Chem. Ref. Data* **1995**, *24*, 663−1021.
(48) Davies, M. J. *Biochem. Biophys. Res. Commun.* **2003**, *305*, 761−770.
(49) Lindig, B. A.; Rodgers, M. A. J. *J. Phys. Chem.* **1979**, *83*, 1683−1688.
(50) Liu, H.-W.; Xu, S.; Wang, P.; Hu, X.-X.; Zhang, J.; Yuan, L.; Zhang, X.-B.; Tan, W. *Chem. Commun.* **2016**, *52*, 12330−12333.
(51) You, Y.; Cho, E. J.; Kwon, H.; Hwang, J.; Lee, S. E. *Chem. Commun.* **2016**, *52*, 780−783.
(52) Gligorovski, S.; Strekowski, R.; Barbati, S.; Vione, D. *Chem. Rev.* **2015**, *115*, 13051−13092.
(53) Wiseman, H.; Halliwell, B. *Biochem. J.* **1996**, *313*, 17−29.
(54) Cadet, J.; Berger, M.; Douki, T.; Ravanat, J. L. *Rev. Physiol. Biochem. Pharmacol.* **1997**, *131*, 1−87.
(55) Liu, F.; Du, J.; Song, D.; Xu, M.; Sun, G. *Chem. Commun.* **2016**, *52*, 4636−4639.
(56) Wang, J.; Liu, Z.; Ren, M.; Kong, X.; Liu, K.; Deng, B.; Lin, W. *Sens. Actuators, B* **2016**, *236*, 60−66.
(57) Nie, H.; Jing, J.; Tian, Y.; Yang, W.; Zhang, R.; Zhang, X. *ACS Appl. Mater. Interfaces* **2016**, *8*, 8991−8997.
(58) Zhang, H.; Liu, J.; Liu, C.; Yu, P.; Sun, M.; Yan, X.; Guo, J. P.; Guo, W. *Biomaterials* **2017**, *133*, 60−69.
(59) Yap, Y. W.; Whiteman, M.; Cheung, N. S. *Cell. Signalling* **2007**, *19*, 219−228.
(60) Chapple, I. L. C. *J. Clin. Periodontol.* **1997**, *24*, 287−296.
(61) Zhang, R.; Zhao, J.; Han, G.; Liu, Z.; Liu, C.; Zhang, C.; Liu, B.; Jiang, C.; Liu, R.; Zhao, T.; Han, M.; Zhang, Z. *J. Am. Chem. Soc.* **2016**, *138*, 3769−3778.
(62) Li, K.; Hou, J.-T.; Yang, J.; Yu, X.-Q. *Chem. Commun.* **2017**, *53*, 5539−5541.
(63) Chen, X.; Lee, K. A.; Ren, X.; Ryu, J. C.; Kim, G.; Ryu, J. H.; Lee, W. J.; Yoon, J. *Nat. Protoc.* **2016**, *11*, 1219−1228.
(64) Wu, Y.; Wang, J.; Zeng, F.; Huang, S.; Huang, J.; Xie, H.; Yu, C.; Wu, S. *ACS Appl. Mater. Interfaces* **2016**, *8*, 1511−1519.
(65) Zhang, Z.; Fan, J.; Cheng, G.; Ghazali, S.; Du, J.; Peng, X. *Sens. Actuators, B* **2017**, *246*, 293−299.
(66) Guo, B.; Nie, H.; Yang, W.; Tian, Y.; Jing, J.; Zhang, X. *Sens. Actuators, B* **2016**, *236*, 459−465.
(67) Feng, Y.; Li, S.; Li, D.; Wang, Q.; Ning, P.; Chen, M.; Tian, X.; Wang, X. *Sens. Actuators, B* **2018**, *254*, 282−290.
(68) Xu, Q.; Heo, C. H.; Kim, J. A.; Lee, H. S.; Hu, Y.; Kim, D.; Swamy, K. M. K.; Kim, G.; Nam, S. J.; Kim, H. M.; Yoon, J. *Anal. Chem.* **2016**, *88*, 6615−6620.
(69) Zhu, B.; Li, P.; Shu, W.; Wang, X.; Liu, C.; Wang, Y.; Wang, Z.; Wang, Y.; Tang, B. *Anal. Chem.* **2016**, *88*, 12532−12538.
(70) Xing, P.; Gao, K.; Wang, B.; Gao, J.; Yan, H.; Wen, J.; Li, W.; Xu, Y.; Li, H.; Chen, J.; Wang, W.; Sun, S. *Chem. Commun.* **2016**, *52*, 5064−5066.
(71) Liang, L.; Liu, C.; Jiao, X.; Zhao, L.; Zeng, X. *Chem. Commun.* **2016**, *52*, 7982−7985.
(72) Tian, F.; Jia, Y.; Zhang, Y.; Song, W.; Zhao, G.; Qu, Z.; Li, C.; Chen, Y.; Li, P. *Biosens. Bioelectron.* **2016**, *86*, 68−74.
(73) Mulay, S. V.; Choi, M.; Jang, Y. J.; Kim, Y.; Jon, S.; Churchill, D. G. *Chem. - Eur. J.* **2016**, *22*, 9642−9648.
(74) Hu, J.; Wong, N.−K.; Lu, M.−Y.; Chen, X.; Ye, S.; Zhao, A. Q.; Gao, P.; Kao, R. Y.−T.; Shen, J.; Yang, D. *Chem. Sci.* **2016**, *7*, 2094−2099.
(75) Zhang, Y.−R.; Zhao, Z.−M.; Miao, J.−Y.; Zhao, B.−X. *Sens. Actuators, B* **2016**, *229*, 408−413.
(76) Li, G.; Ji, D.; Zhang, S.; Li, J.; Li, C.; Qiao, R. *Sens. Actuators, B* **2017**, *252*, 127−133.
(77) McCall, A. S.; Cummings, C. F.; Bhave, G.; Vanacore, R.; PageMcCaw, A.; Hudson, B. G. *Cell* **2014**, *157*, 1380−1392.
(78) Xu, K.; Luan, D.; Wang, X.; Hu, B.; Liu, X.; Kong, F.; Tang, B. *Angew. Chem., Int. Ed.* **2016**, *55*, 12751−12754.
(79) Liu, X.; Zheng, A.; Luan, D.; Wang, X.; Kong, F.; Tong, L.; Xu, K.; Tang, B. *Anal. Chem.* **2017**, *89*, 1787−1792.
(80) Radi, R. *J. Biol. Chem.* **2013**, *288*, 26464−26472.
(81) Ferrer-Sueta, G.; Radi, R. *ACS Chem. Biol.* **2009**, *4*, 161−177.
(82) Peng, T.; Chen, X.; Gao, L.; Zhang, T.; Wang, W.; Shen, J.; Yang, D. *Chem. Sci.* **2016**, *7*, 5407−5413.
(83) Zhao, C.; An, J.; Zhou, L.; Fei, Q.; Wang, F.; Tan, J.; Shi, B.; Wang, R.; Guo, Z.; Zhu, W.−H. *Chem. Commun.* **2016**, *52*, 2075−2078.
(84) Li, J.; Lim, C. S.; Kim, G.; Kim, H. M.; Yoon, J. *Anal. Chem.* **2017**, *89*, 8496−8500.
(85) Sedgwick, A. C.; Sun, X.; Kim, G.; Yoon, J.; Bull, S. D.; James, T. D. *Chem. Commun.* **2016**, *52*, 12350−12352.
(86) Rios, N.; Piacenza, L.; Trujillo, M.; Martínez, A.; Demicheli, V.; Prolo, C.; Álvarez, M. N.; López, G. V.; Radi, R. *Free Radical Biol. Med.* **2016**, *101*, 284−295.

DOI: 10.1021/acs.analchem.7b04234
Anal. Chem. 2018, 90, 533−555

(87) Zhang, J.; Li, Y. P.; Zhao, J. J.; Guo, W. *Sens. Actuators, B* **2016**, *237*, 67−74.
(88) Jia, X.; Chen, Q.; Yang, Y.; Tang, Y.; Wang, R.; Xu, Y.; Zhu, W.; Qian, X. *J. Am. Chem. Soc.* **2016**, *138*, 10778−10781.
(89) Li, Z.; Yan, S.−H.; Chen, C.; Geng, Z.−R.; Chang, J.−Y.; Chen, C.−X.; Huang, B. − H.; Wang, Z.−L. *Biosens. Bioelectron.* **2017**, *90*, 75−82.
(90) Li, Y.; Xie, X.; Yang, X.; Li, M.; Jiao, X.; Sun, Y.; Wang, X.; Tang, B. *Chem. Sci.* **2017**, *8*, 4006−4011.
(91) Cheng, D.; Xu, W.; Yuan, L.; Zhang, X. *Anal. Chem.* **2017**, *89*, 7693−7700.
(92) Miao, J.; Huo, Y.; Liu, Q.; Li, Z.; Shi, H.; Shi, Y.; Guo, W. *Biomaterials* **2016**, *107*, 33−43.
(93) Cheng, D.; Pan, Y.; Wang, L.; Zeng, Z.; Yuan, L.; Zhang, X.; Chang, Y.−T. *J. Am. Chem. Soc.* **2017**, *139*, 285−292.
(94) Li, H.; Li, X.; Wu, X.; Shi, W.; Ma, H. *Anal. Chem.* **2017**, *89*, 5519−5525.
(95) Rivera-Fuentes, P.; Lippard, S. J. *Acc. Chem. Res.* **2015**, *48*, 2927−2934.
(96) Snyder, S. H. *Science* **1992**, *257*, 494−496.
(97) Wang, P. G.; Xian, M.; Tang, X.; Wu, X.; Wen, Z.; Cai, T.; Janczuk, A. J. *Chem. Rev.* **2002**, *102*, 1091−1134.
(98) Zhang, H.−X.; Chen, J.−B.; Guo, X.−F.; Wang, H.; Zhang, H.−S. *Anal. Chem.* **2014**, *86*, 3115−3123.
(99) Mao, Z.; Feng, W.; Li, Z.; Zeng, L.; Lv, W.; Liu, Z. *Chem. Sci.* **2016**, *7*, 5230−5235.
(100) Yao, H.−W.; Zhu, X.−Y.; Guo, X.−F.; Wang, H. *Anal. Chem.* **2016**, *88*, 9014−9021.
(101) Wang, B.; Yu, S.; Chai, X.; Li, T.; Wu, Q.; Wang, T. *Chem. - Eur. J.* **2016**, *22*, 5649−5656.
(102) Huo, Y.; Miao, J.; Han, L.; Li, Y.; Li, Z.; Shi, Y.; Guo, W. *Chem. Sci.* **2017**, *8*, 6857−6864.
(103) Miao, J.; Huo, Y.; Lv, X.; Li, Z.; Cao, H.; Shi, H.; Shi, Y.; Guo, W. *Biomaterials* **2016**, *78*, 11−19.
(104) Mao, Z.; Jiang, H.; Li, Z.; Zhong, C.; Zhang, W.; Liu, Z. *Chem. Sci.* **2017**, *8*, 4533−4538.
(105) Li, H.; Zhang, D.; Gao, M.; Huang, L.; Tang, L.; Li, Z.; Chen, X.; Zhang, X. *Chem. Sci.* **2017**, *8*, 2199−2203.
(106) Zhou, Y.; Zhang, X.; Yang, S.; Li, Y.; Qing, Z.; Zheng, J.; Li, J.; Yang, R. *Anal. Chem.* **2017**, *89*, 4587−4594.
(107) Zheng, K.; Chen, H.; Fang, S.; Wang, Y. *Sens. Actuators, B* **2016**, *233*, 193−198.
(108) Sunwoo, K.; Bobba, K. N.; Lim, J.-Y.; Park, T.; Podder, A.; Heo, J. S.; Lee, S. G.; Bhuniya, S.; Kim, J. S. *Chem. Commun.* **2017**, *53*, 1723−1726.
(109) Zhu, X.; Xiong, M.; Liu, H.−W.; Mao, G.−J.; Zhou, L.; Zhang, J.; Hu, X.; Zhang, X. − B.; Tan, W. *Chem. Commun.* **2016**, *52*, 733−736.
(110) Shao, S.; Chen, B.; Cheng, J.; Wang, C.; Zhang, Y.; Shao, L.; Hu, Y.; Han, Y.; Han, F.; Li, X. *Biosens. Bioelectron.* **2017**, *94*, 162−168.
(111) Giles, N. M.; Watts, A. B.; Giles, G. I.; Fry, F. H.; Littlechild, J. A.; Jacob, C. *Chem. Biol.* **2003**, *10*, 677−693.
(112) Umezawa, K.; Yoshida, M.; Kamiya, M.; Yamasoba, T.; Urano, Y. *Nat. Chem.* **2017**, *9*, 279−286.
(113) Liu, Z.; Zhou, X.; Miao, Y.; Hu, Y.; Kwon, N.; Wu, X.; Yoon, J. *Angew. Chem., Int. Ed.* **2017**, *56*, 5812−5816.
(114) Xie, J.−Y.; Li, C.−Y.; Li, Y.−F.; Fei, J.−J.; Xu, F.; Ou-Yang, J. O.; Liu, J. *Anal. Chem.* **2016**, *88*, 9746−9752.
(115) Huang, R.; Wang, B.−B.; Si-Tu, X − M.; Gao, T.; Wang, F.−F.; He, H.; Fan, X.−Y.; Jiang, F − L.; Liu, Y. *Chem. Commun.* **2016**, *52*, 11579−11582.
(116) Zhang, H.; Wang, C.; Wang, G.; Wang, K.; Jiang, K. *Biosens. Bioelectron.* **2016**, *78*, 344−350.
(117) Zhang, H.; Wang, C.; Wang, K.; Xuan, X.; Lv, Q.; Jiang, K. *Biosens. Bioelectron.* **2016**, *85*, 96−102.
(118) Cao, M.; Chen, H.; Chen, D.; Xu, Z.; Liu, S.−H.; Chen, X.; Yin, J. *Chem. Commun.* **2016**, *52*, 721−724.
(119) Lehmann, A. *Neuroscience* **1987**, *22*, 573−578.
(120) Heafield, M. T.; Fearn, S.; Steventon, G. B.; Waring, R. H.; Williams, A. C.; Sturman, S. G. *Neurosci. Lett.* **1990**, *110*, 216−220.
(121) Tong, H.; Zhao, J.; Li, X.; Zhang, Y.; Ma, S.; Lou, K.; Wang, W. *Chem. Commun.* **2017**, *53*, 3583−3586.
(122) Liu, T.; Huo, F.; Li, J.; Chao, J.; Zhang, Y.; Yin, C. *Sens. Actuators, B* **2016**, *237*, 127−132.
(123) Wang, J.; Li, B.; Zhao, W.; Zhang, X.; Luo, X.; Corkins, M. E.; Cole, S. L.; Wang, C.; Xiao, Y.; Bi, X.; Pang, Y.; McElroy, C. A.; Bird, A. J.; Dong, Y. Z. *ACS Sens.* **2016**, *1*, 882−887.
(124) Ma, W.−W.; Wang, M.−Y.; Yin, D.; Zhang, X. *Sens. Actuators, B* **2017**, *248*, 332−337.
(125) Kim, C. Y.; Kang, H. J.; Chung, S. J.; Kim, H.−K.; Na, S.−Y.; Kim, H.−J. *Anal. Chem.* **2016**, *88*, 7178−7182.
(126) Niu, W.; Guo, L.; Li, Y.; Shuang, S.; Dong, C.; Wong, M. S. *Anal. Chem.* **2016**, *88*, 1908−1914.
(127) Anila, H. A.; Ali, F.; Kushwaha, S.; Taye, N.; Chattopadhyay, S.; Das, A. *Anal. Chem.* **2016**, *88*, 12161−12168.
(128) Fu, Z.−H.; Han, X.; Shao, Y.; Fang, J.; Zhang, Z.−H.; Wang, Y.−W.; Peng, Y. *Anal. Chem.* **2017**, *89*, 1937−1944.
(129) Rani, B. K.; John, S. A. *Biosens. Bioelectron.* **2016**, *83*, 237−242.
(130) He, X.; Wu, X.; Shi, W.; Ma, H. *Chem. Commun.* **2016**, *52*, 9410−9413.
(131) Yue, Y.; Huo, F.; Ning, P.; Zhang, Y.; Chao, J.; Meng, X.; Yin, C. *J. Am. Chem. Soc.* **2017**, *139*, 3181−3185.
(132) Gong, D.; Tian, Y.; Yang, C.; Iqbal, A.; Wang, Z.; Liu, W.; Qin, W.; Zhu, X.; Guo, H. *Biosens. Bioelectron.* **2016**, *85*, 178−183.
(133) Wang, Y.−W.; Liu, S.−B.; Ling, W.−J.; Peng, Y. *Chem. Commun.* **2016**, *52*, 827−830.
(134) Chen, W.; Luo, H.; Liu, X.; Foley, J. W.; Song, X. *Anal. Chem.* **2016**, *88*, 3638−3646.
(135) Hu, Q.; Yu, C.; Xia, X.; Zeng, F.; Wu, S. *Biosens. Bioelectron.* **2016**, *81*, 341−348.
(136) Wang, K.; Leng, T.; Liu, Y.; Wang, C.; Shi, P.; Shen, Y.; Zhu, W.−H. *Sens. Actuators, B* **2017**, *248*, 338−345.
(137) Chen, H.; Tang, Y.; Ren, M.; Lin, W. *Chem. Sci.* **2016**, *7*, 1896−1903.
(138) Dai, X.; Zhang, T.; Miao, J.−Y.; Zhao, B.−X. *Sens. Actuators, B* **2016**, *223*, 274−279.
(139) Liu, K.; Shang, H.; Kong, X.; Lin, W. *J. Mater. Chem. B* **2017**, *5*, 3836−3841.
(140) Xie, X.; Li, M.; Tang, F.; Li, Y.; Zhang, L.; Jiao, X.; Wang, X.; Tang, B. *Anal. Chem.* **2017**, *89*, 3015−3020.
(141) Li, Y.; Liu, W.; Zhang, P.; Zhang, H.; Wu, J.; Ge, J.; Wang, P. *Biosens. Bioelectron.* **2017**, *90*, 117−124.
(142) Zhang, H.; Liu, R.; Liu, J.; Li, L.; Wang, P.; Yao, S. Q.; Xu, Z.; Sun, H. *Chem. Sci.* **2016**, *7*, 256−260.
(143) Li, L.; Rose, P.; Moore, P. K. *Annu. Rev. Pharmacol. Toxicol.* **2011**, *51*, 169−187.
(144) Dorman, D. C.; Moulin, F. J.-M.; McManus, B. E.; Mahle, K. C.; James, R. A.; Struve, M. F. *Toxicol. Sci.* **2002**, *65*, 18−25.
(145) Liu, Y.-H.; Lu, M.; Hu, L.-F.; Wong, P. T.-H.; Webb, G. D.; Bian, J.-S. *Antioxid. Redox Signaling* **2012**, *17*, 141−185.
(146) Papapetropoulos, A.; Pyriochou, A.; Altaany, Z.; Yang, G.; Marazioti, A.; Zhou, Z.; Jeschke, M. G.; Branski, L. K.; Herndon, D. N.; Wang, R. *Proc. Natl. Acad. Sci. U. S. A.* **2009**, *106*, 21972−21977.
(147) Módis, K.; Ju, Y.; Ahmad, A.; Untereiner, A. A.; Altaany, Z.; Wu, L.; Szabo, C.; Wang, R. *Pharmacol. Res.* **2016**, *113*, 116−124.
(148) Wallace, J. L. *Trends Pharmacol. Sci.* **2007**, *28*, 501−505.
(149) Feng, X.; Zhang, T.; Liu, J.-T.; Miao, J.-Y.; Zhao, B.-X. *Chem. Commun.* **2016**, *52*, 3131−3134.
(150) Ren, M.; Deng, B.; Kong, X.; Zhou, K.; Liu, K.; Xu, G.; Lin, W. *Chem. Commun.* **2016**, *52*, 6415−6418.
(151) Liu, Y.; Meng, F.; He, L.; Liu, K.; Lin, W. *Chem. Commun.* **2016**, *52*, 7016−7019.
(152) He, L.; Yang, X.; Xu, K.; Kong, X.; Lin, W. *Chem. Sci.* **2017**, *8*, 6257−6265.
(153) Li, H.; Peng, W.; Feng, W.; Wang, Y.; Chen, G.; Wang, S.; Li, S.; Li, H.; Wang, K.; Zhang, J. *Chem. Commun.* **2016**, *52*, 4628−4631.
(154) Pak, Y. L.; Li, J.; Ko, K. C.; Kim, G.; Lee, J. Y.; Yoon, J. *Anal. Chem.* **2016**, *88*, 5476−5481.

DOI: 10.1021/acs.analchem.7b04234
Anal. Chem. 2018, 90, 533−555

(155) Kang, J.; Huo, F.; Ning, P.; Meng, X.; Chao, J.; Yin, C. *Sens. Actuators, B* **2017**, *250*, 342−350.
(156) Zhang, K.; Zhang, J.; Xi, Z.; Li, L.-Y.; Gu, X.; Zhang, Q.-Z.; Yi, L. *Chem. Sci.* **2017**, *8*, 2776−2781.
(157) Jin, X.; Wu, S.; She, M.; Jia, Y.; Hao, L.; Yin, B.; Wang, L.; Obst, M.; Shen, Y.; Zhang, Y. *Anal. Chem.* **2016**, *88*, 11253−11260.
(158) Karakuş, E.; Üçüncü, M.; Emrullahoğlu, M. *Anal. Chem.* **2016**, *88*, 1039−1043.
(159) Reja, S. I.; Sharma, N.; Gupta, M.; Bajaj, P.; Bhalla, V.; Parihar, R. D.; Ohri, P.; Kaur, G.; Kumar, M. S. *Chem. - Eur. J.* **2017**, *23*, 9872−9878.
(160) Lv, J.; Wang, F.; Qiang, J.; Ren, X.; Chen, Y.; Zhang, Z.; Wang, Y.; Zhang, W.; Chen, X. *Biosens. Bioelectron.* **2017**, *87*, 96−100.
(161) Wu, Z.; Liang, D.; Tang, X. *Anal. Chem.* **2016**, *88*, 9213−9218.
(162) Velusamy, N.; Binoy, A.; Bobba, K. N.; Nedungadi, D.; Mishra, N.; Bhuniya, S. *Chem. Commun.* **2017**, *53*, 8802−8805.
(163) Deng, B.; Ren, M.; Wang, J.-Y.; Zhou, K.; Lin, W. *Sens. Actuators, B* **2017**, *248*, 50−56.
(164) Wang, S.; Xu, S.; Hu, G.; Bai, X.; James, T. D.; Wang, L. *Anal. Chem.* **2016**, *88*, 1434−1439.
(165) Chen, L.; Wu, D.; Lim, C. S.; Kim, D.; Nam, S.-J.; Lee, W.; Kim, G.; Kim, H. M.; Yoon, J. *Chem. Commun.* **2017**, *53*, 4791−4794.
(166) Gong, D.; Zhu, X.; Tian, Y.; Han, S.-C.; Deng, M.; Iqbal, A.; Liu, W.; Qin, W.; Guo, H. *Anal. Chem.* **2017**, *89*, 1801−1807.
(167) Toohey, J. I. *Anal. Biochem.* **2011**, *413*, 1−7.
(168) Vitvitsky, V.; Kabil, O.; Banerjee, R. *Antioxid. Redox Signaling* **2012**, *17*, 22−31.
(169) Greiner, R.; Pálinkás, Z.; Bäsell, K.; Becher, D.; Antelmann, H.; Nagy, P.; Dick, T. P. *Antioxid. Redox Signaling* **2013**, *19*, 1749−1765.
(170) Chen, W.; Pacheco, A.; Takano, Y.; Day, J. J.; Hanaoka, K.; Xian, M. *Angew. Chem., Int. Ed.* **2016**, *55*, 9993−9996.
(171) Fang, Y.; Chen, W.; Shi, W.; Li, H.; Xian, M.; Ma, H. *Chem. Commun.* **2017**, *53*, 8759−8762.
(172) Han, Q.; Mou, Z.; Wang, H.; Tang, X.; Dong, Z.; Wang, L.; Dong, X.; Liu, W. *Anal. Chem.* **2016**, *88*, 7206−7212.
(173) Zhang, J.; Zhu, X.-Y.; Hu, X.-X.; Liu, H.-W.; Li, J.; Feng, L.-L.; Yin, X.; Zhang, X.-B.; Tan, W. *Anal. Chem.* **2016**, *88*, 11892−11899.
(174) Li, K.-B.; Chen, F.-Z.; Yin, Q.-H.; Zhang, S.; Shi, W.; Han, D.-M. *Sens. Actuators, B* **2018**, *254*, 222−226.
(175) Takano, Y.; Hanaoka, K.; Shimamoto, K.; Miyamoto, R.; Komatsu, T.; Ueno, T.; Terai, T.; Kimura, H.; Nagano, T.; Urano, Y. *Chem. Commun.* **2017**, *53*, 1064−1067.
(176) Huang, Y.; Yu, F.; Wang, J.; Chen, L. *Anal. Chem.* **2016**, *88*, 4122−4129.
(177) Ida, T.; Sawa, T.; Ihara, H.; Tsuchiya, Y.; Watanabe, Y.; Kumagai, Y.; Suematsu, M.; Motohashi, H.; Fujii, S.; Matsunaga, T. *Proc. Natl. Acad. Sci. U. S. A.* **2014**, *111*, 7606−7611.
(178) Luebke, J. L.; Shen, J.; Bruce, K. E.; Kehl-Fie, T. E.; Peng, H.; Skaar, E. P.; Giedroc, D. P. *Mol. Microbiol.* **2014**, *94*, 1343−1360.
(179) Han, X.; Yu, F.; Song, X.; Chen, L. *Chem. Sci.* **2016**, *7*, 5098−5107.
(180) Kawagoe, R.; Takashima, I.; Uchinomiya, S.; Ojida, A. *Chem. Sci.* **2017**, *8*, 1134−1140.
(181) Meng, Z.; Qin, G.; Zhang, B.; Bai, J. *Mutagenesis* **2004**, *19*, 465−468.
(182) Shi, X. *J. Inorg. Biochem.* **1994**, *56*, 155−165.
(183) Chen, T.-M.; Gokhale, J.; Shofer, S.; Kuschner, W. G. *Am. J. Med. Sci.* **2007**, *333*, 249−256.
(184) Sang, N.; Yun, Y.; Li, H.; Hou, L.; Han, M.; Li, G. *Toxicol. Sci.* **2010**, *114*, 226−236.
(185) Tang, L.; He, P.; Yan, X.; Sun, J.; Zhong, K.; Hou, S.; Bian, Y. *Sens. Actuators, B* **2017**, *247*, 421−427.
(186) Li, D.; Shi, Y.; Tian, X.; Wang, M.; Huang, B.; Li, F.; Li, S.; Zhou, H.; Wu, J.; Tian, Y. *Sens. Actuators, B* **2016**, *233*, 1−6.
(187) Xu, J.; Pan, J.; Jiang, X.; Qin, C.; Zeng, L.; Zhang, H.; Zhang, J. F. *Biosens. Bioelectron.* **2016**, *77*, 725−732.
(188) Liu, Y.; Li, K.; Xie, K.-X.; Li, L.-L.; Yu, K.-K.; Wang, X.; Yu, X.-Q. *Chem. Commun.* **2016**, *52*, 3430−3433.
(189) Xu, W.; Ma, P.; Diao, Q.; Xu, L.; Liu, X.; Sun, Y.; Wang, X.; Song, D. *Sens. Actuators, B* **2017**, *252*, 86−94.
(190) Li, D.-P.; Wang, Z.-Y.; Cao, X.-J.; Cui, J.; Wang, X.; Cui, H.-Z.; Miao, J.-Y.; Zhao, B.-X. *Chem. Commun.* **2016**, *52*, 2760−2763.
(191) Li, D.-P.; Wang, Z.-Y.; Su, H.; Miao, J.-Y.; Zhao, B.-X. *Chem. Commun.* **2017**, *53*, 577−580.
(192) Yang, X.; Zhou, Y.; Zhang, X.; Yang, S.; Chen, Y.; Guo, J.; Li, X.; Qing, Z.; Yang, R. *Chem. Commun.* **2016**, *52*, 10289−10292.
(193) Zhang, Y.; Guan, L.; Yu, H.; Yan, Y.; Du, L.; Liu, Y.; Sun, M.; Huang, D.; Wang, S. *Anal. Chem.* **2016**, *88*, 4426−4431.
(194) Zhang, W.; Liu, T.; Huo, F.; Ning, P.; Meng, X.; Yin, C. *Anal. Chem.* **2017**, *89*, 8079−8083.
(195) Samanta, S.; Dey, P.; Ramesh, A.; Das, G. *Chem. Commun.* **2016**, *52*, 10381−10384.
(196) Dou, K.; Fu, Q.; Chen, G.; Yu, F.; Liu, Y.; Cao, Z.; Li, G.; Zhao, X.; Xia, L.; Chen, L.; Wang, H.; You, J. *Biomaterials* **2017**, *133*, 82−93.
(197) Yu, S.; Yang, X.; Shao, Z.; Feng, Y.; Xi, X.; Shao, R.; Guo, Q.; Meng, X. *Sens. Actuators, B* **2016**, *235*, 362−369.
(198) Hondal, R. J.; Nilsson, B. L.; Raines, R. T. *J. Am. Chem. Soc.* **2001**, *123*, 5140−5141.
(199) Du, X.; Wang, C.; Liu, Q. *Curr. Top. Med. Chem.* **2016**, *16*, 835−848.
(200) Fairweather-Tait, S. J.; Bao, Y.; Broadley, M. R.; Collings, R.; Ford, D.; Hesketh, J. E.; Hurst, R. *Antioxid. Redox Signaling* **2011**, *14*, 1337−1383.
(201) Battin, E. E.; Brumaghim, J. L. *Cell Biochem. Biophys.* **2009**, *55*, 1−23.
(202) Wallenberg, M.; Olm, E.; Hebert, C.; Björnstedt, M.; Fernandes, A. P. *Biochem. J.* **2010**, *429*, 85−93.
(203) Sun, Q.; Yang, S.-H.; Wu, L.; Dong, Q.-J.; Yang, W.-C.; Yang, G.-F. *Anal. Chem.* **2016**, *88*, 6084−6091.
(204) Feng, W.; Li, M.; Sun, Y.; Feng, G. *Anal. Chem.* **2017**, *89*, 6106−6112.
(205) Han, X.; Song, X.; Yu, F.; Chen, L. *Adv. Funct. Mater.* **2017**, *27*, 1700769.
(206) Kong, F.; Ge, L.; Pan, X.; Xu, K.; Liu, X.; Tang, B. *Chem. Sci.* **2016**, *7*, 1051−1056.
(207) Kong, F.; Zhao, Y.; Liang, Z.; Liu, X.; Pan, X.; Luan, D.; Xu, K.; Tang, B. *Anal. Chem.* **2017**, *89*, 688−693.
(208) Antaris, A. L.; Chen, H.; Cheng, K.; Sun, Y.; Hong, G.; Qu, C.; Diao, S.; Deng, Z.; Hu, X.; Zhang, B.; Zhang, X.; Yaghi, O. K.; Alamparambil, Z. R.; Hong, X.; Cheng, Z.; Dai, H. *Nat. Mater.* **2016**, *15*, 235−242.
(209) Cho, A.; Choi, K. *Chem. Lett.* **2012**, *41*, 1611−1612.
(210) Kim, I.-G.; Choi, K.; Jeong, E. M.; Kang, H. S. WO2016080759A2, 2016.

DOI: 10.1021/acs.analchem.7b04234
Anal. Chem. 2018, 90, 533−555